Optimising Industrial Buildings in India

A calibrated building performance simulation case study

Ishaan Vinay Mahajan

Master thesis in Energy-efficient and Environmental Buildings
Faculty of Engineering | Lund University

Lund University

Lund University, with eight faculties and a number of research centres and specialized institutes, is the largest establishment for research and higher education in Scandinavia. The main part of the University is situated in the small city of Lund which has about 112 000 inhabitants. A number of departments for research and education are, however, located in Malmö. Lund University was founded in 1666 and has today a total staff of 6 000 employees and 47 000 students attending 280 degree programmes and 2 300 subject courses offered by 63 departments.

Master Programme in Energy-efficient and Environmental Building Design

This international programme provides knowledge, skills and competencies within the area of energy-efficient and environmental building design in cold climates. The goal is to train highly skilled professionals, who will significantly contribute to and influence the design, building or renovation of energy-efficient buildings, taking into consideration the architecture and environment, the inhabitants' behaviour and needs, their health and comfort as well as the overall economy.

The degree project is the final part of the master programme leading to a Master of Science (120 credits) in Energy-efficient and Environmental Buildings.

Examiner: Jouri Kanters (Division of Energy and Building Design, Department of Building and Environmental Technology, Lund University)

Supervisor: Pieter de Wilde (Division of Energy and Building Design, Department of Building and Environmental Technology, Lund University)

Keywords: Industrial Buildings, Energy Use Intensity, Thermal Comfort, Parametric Simulations, Adaptive Comfort

Publication year: 2026

Abstract

India's buildings sector accounts for 41% of national electricity consumption, yet studies incorporating calibrated whole-building energy simulation with thermal comfort evaluation of manufacturing facilities to reduce the industry's electricity consumption remain scarce, leaving designers without evidence to prioritise passive strategies for this building typology. This study characterises the energy use intensity (EUI) and worker thermal comfort of five manufacturing buildings, at a truck production facility in Bhopal (composite climate zone), through 1,925 parametric simulations across seven design and operational variables, evaluated against an 18-metric comfort framework integrating the Indian Model for Adaptive Comfort (IMAC) and Standard Effective Temperature (SET) across three airspeed levels.

Across all five buildings, the EUI can be grouped into distinct performance bands based on three parameters: lighting power density (LPD), roof insulation, and shift scheduling, which together produce mean reductions up to 20 kWh/m²/year, while the remaining four variables (wall insulation, window specification, skylight type, and solar absorptance) produce within band movement without shifting a building between tiers. Thermal comfort responds differently: HVLS fan operation at the first airspeed threshold reduces discomfort hours by up to 26%, more than all envelope measures combined, naturally ventilated buildings show broad alignment between low EUI and low discomfort scenarios, whereas process dominated buildings remain in persistent discomfort across all scenarios. The as built design already approaches the parametric optimum within 2%, but worst case specification raises EUI by 14% to 27%.

Declaration of generative AI and AI-assisted technologies in the writing process

The content of this thesis is created by the author; however, Perplexity was used to generate codes for simulations and visualisations, and to improve readability. After using this tool, the author reviewed and edited the content as needed and take full responsibility for the content of the publication

Acknowledgements

I would like to express my sincere gratitude to my supervisor, Pieter de Wilde, of the Division of Energy and Building Design at Lund University, for his guidance, insights, and consistent support throughout this research. His role in helping me identify and shape this research topic, along with his expertise in building performance simulation were instrumental in defining the direction and methodology of this thesis.

I am also grateful to my examiner, Jouri Kanters, whose feedback helped sharpen the clarity and significance of this work.

This thesis would not have been possible without the cooperation of the teams at the truck manufacturing facility in Bhopal. I extend my thanks to the architects, lighting consultants, facility managers, and client representatives who provided drawings, specifications, energy data, and access during the site visit. Their willingness to share operational knowledge of a live industrial facility was invaluable.

Finally, I am deeply grateful to my family, whose unwavering support and encouragement have been a constant source of strength throughout my studies.

Table of Contents

1 INTRODUCTION

The global built environment stands at the centre of the climate crisis. In 2022, the buildings and construction sector accounted for approximately 34% of total global final energy demand and 37% of energy and process related CO_2 emissions, reaching a new peak of just under 10 $GtCO_2$ (International Energy Agency, 2023; United Nations Environment Programme, 2024). Operational energy demand consumed 30% of global final energy, with a further 4% attributable to the production of construction materials such as cement, steel, and aluminium (United Nations Environment Programme, 2024). Despite a 3.5% improvement in energy intensity per square metre in buildings between 2021 and 2022, overall sectoral emissions still grew by approximately 1%, highlighting the inadequacy of current efficiency gains relative to the pace of construction (United Nations Environment Programme, 2024).

The scale of the problem is compounded by the trajectory of future construction. Approximately 60% of the buildings that will exist by 2050 have not yet been built, with majority of new floor space concentrated in emerging and developing economies (International Energy Agency, 2018; United Nations Environment Programme, 2024). A significant share of future additions are projected in hot climate regions that currently lack comprehensive building energy codes, creating a critical risk of building a thermally inefficient building stock for decades (United Nations Environment Programme, 2024). There is an urgency in decarbonising buildings globally, if new construction in developing economies is designed efficiently from the outset, a significant share of projected global energy demand growth can be avoided (Energy Transitions Commission, 2020; International Energy Agency, 2021b; United Nations Environment Programme, 2024).

Policy ambition has grown, 28 countries committed to the Buildings Breakthrough at COP28, targeting near zero emission and resilient buildings by 2030, but the Global Buildings Climate Tracker shows that actual decarbonisation progress remains far off the required path (United Nations Environment Programme, 2024). Annual CO_2 reductions of approximately 10% per year until 2030 are now required to realign with the IEA Net Zero Emissions scenario (United Nations Environment Programme, 2024).

1.1 India’s industrial Building Energy Context

India exemplifies the intersection of rapid economic growth, surging energy demand, and the urgent need for efficient built environments. Buildings account for approximately 41% of India's total energy consumption, a figure growing at around 8% annually (International Energy Agency, 2021a; United Nations Environment Programme, 2024). The industrial sector, which includes manufacturing facilities, accounts for approximately 32% of total national electricity consumption, with industrial electricity use rising by 30% in three years from 283 billion units in FY2021 to 368 billion units in FY2024 (Michael et al., 2025). India's manufacturing real estate is expanding; manufacturing leasing reached 22.1 million sq. ft in 2024 and is projected to reach 34 million sq. ft by 2027, representing 46% of India's total real estate stock, driven by the automotive, electronics, and engineering sectors under the Make in India policy (Sharma, 2025). Grade A manufacturing facility demand has grown sharply, rising from 70% of total absorption in 2019 to 87% by Q3 2025, reflecting increasing requirements for high end specifications, automation readiness, and sustainability compliance (Sharma, 2025).

This expansion of manufacturing floor space is accompanied by a projected 45% rise in heavy industry electricity demand, from 175 TWh in 2022 to 253 TWh by 2030, driven by growth in steel, aluminium, and cement sectors (Das & Lolla, 2024). Decarbonising this electricity demand through renewable energy sources would require approximately 120 GW of additional renewable capacity by 2030 and could avoid 180 Mt of CO_2 emissions annually (Das & Lolla, 2024). India's broader policy response, including the Rs 20 lakh crore stimulus package that explicitly prioritised clean energy and domestic manufacturing resilience, reflects a national strategy to leverage this industrial growth as a catalyst for clean energy transition (Government of India, 2020; NITI Aayog & Rocky Mountain Institute (RMI), 2020).

India's urbanisation is the central structural driver of this broader trajectory. An estimated 270 million people are projected to be added to India's urban population by 2040, and two thirds of the buildings that will exist in India by 2040 have not yet been constructed (International Energy Agency, 2021a). The share of buildings in India's total electricity consumption is projected to rise from 41% in 2019 to 48% by 2040 as appliance ownership grows rapidly (International Energy Agency, 2021a). India experiences 28% of the global share of population weighted annual Cooling Degree Days while simultaneously having less than 7% residential air conditioner penetration, creating an imminent and large scale surge in cooling energy demand (International Energy Agency, 2021a).

The built environment and manufacturing sector thus face a dual challenge: meeting growing demands for thermal comfort and productivity while constraining the associated energy and carbon footprint. India attributed 40% of its CO_2 emissions to buildings and enacted legislation to initiate carbon trading and sustainable building codes (United Nations Environment Programme, 2024). The India Cooling Action Plan (ICAP), launched in 2019, sets a target to reduce cooling energy requirements by 25% - 40% by 2037 - 38, identifying thermally efficient building design as a primary instrument (Government of India, 2019). However, policy implementation in industrial buildings, which combine large volume naturally ventilated spaces with process heat loads and multi shift operations, remains limited, and evidence of practical building scale interventions in this context is scarce. No studies integrating calibrated energy simulation with multi-building thermal comfort evaluation for Indian industrial facilities were identified in a search of Web of Science, Scopus, and Google Scholar.

1.2 Research Gap

Within the broader buildings' literature, industrial and manufacturing facilities constitute a distinct and relatively understudied building typology. Unlike offices or residences; for which building energy codes, comfort standards, and efficiency retrofit programmes are well developed, industrial buildings are characterised by large high bay volumes, dominant roof driven heat gain, significant process generated internal loads, variable multi shift occupancy, and operational requirements that are incompatible with conventional sealed HVAC approaches (American Society of Heating, Refrigerating and Air-Conditioning Engineers, 2016). Most existing building energy research in India addresses commercial or residential typologies; industrial facilities, despite accounting for the largest share of national energy use, remain outside the scope of most building level efficiency studies (Kumar et al., 2021; Manu et al., 2016).

The evidence base on passive and low energy strategies for Indian industrial buildings is fragmented. Studies that do exist are typically limited to a single building type, a single season, or a single intervention tested under experimental rather than operational conditions (Kumar et al., 2021; Verma et al., 2026). Critically, these studies have not been connected to calibrated whole building energy simulation, making it difficult to translate isolated experimental findings into verified energy savings or to compare the relative contribution of envelope, ventilation, and lighting strategies within an actual facility.

The thermal comfort dimension compounds this gap. Workers in manufacturing environments operate at substantially higher metabolic rates than the sedentary office occupants for whom international standards such as ASHRAE 55 and EN 16798-1 were designed, and they rely primarily on natural ventilation, ceiling fans, and evaporative cooling rather than mechanical air conditioning (American Society of Heating, Refrigerating and Air-Conditioning Engineers, 2013). India specific comfort research has established that Indian building occupants are significantly more thermally adaptive than international standards predict and field studies in Indian factory and workshop buildings have confirmed that this adaptivity extends to industrial workers at elevated activity levels (Kumar et al., 2020, 2021; Manu et al., 2016; Rawal et al., 2022). However, no dedicated thermal comfort standard exists for Indian industrial workers, and no study identified in this review has integrated a comfort evaluation framework with a calibrated energy model across multiple co located manufacturing building typologies within a single Indian facility (American Society of Heating, Refrigerating and Air-Conditioning Engineers, 2013; International Organization for Standardization (ISO), 2005).

1.3 Aim, Research Questions, and Scope

This thesis aims to characterise the energy use intensity and thermal comfort environment of five manufacturing buildings at a single industrial facility in Bhopal, Madhya Pradesh, and to identify which design and operational strategies most effectively reduce energy consumption while maintaining or improving thermal comfort for workers. The five buildings studied (Machine Shop, Engine Shop, Weld Shop, Cab Trim Shop, and Chassis Assembly Shop) cover a range of building typologies, process types, and cooling strategies, enabling an embedded comparative analysis within a single consistent climatic and operational context.

The primary research question is:

How can building scale design and operational interventions be prioritised to simultaneously reduce energy use intensity and improve thermal comfort for workers across the five manufacturing buildings of an Indian industrial facility in a composite climate?

This is addressed through five sub questions:

1. What are the baseline energy use intensity and thermal comfort profiles of each building, and how do they compare across the five manufacturing typologies?
2. Which energy strategies have the greatest independent effect on EUI and thermal comfort outcomes, and do these effects vary by building typology?
3. What is the effect of operational scheduling (shift timing) and lighting power density on the total energy use of each building?
4. Are there trade-offs between energy reduction and thermal comfort improvement across the parametric scenarios, or do the two objectives generally align?
5. What design recommendations can be derived from the parametric evidence to guide energy efficiency decisions in similar Indian industrial facilities?

The scope of the study is limited to building scale passive and low energy strategies and does not address process energy, production planning, or active mechanical systems beyond the evaporative cooling equipment already installed in the facility. The study is conducted for a single facility in a single climate zone.

2 METHODOLOGY

This chapter describes the methodological framework of the study, covering case study selection, data collection, energy modelling, parametric design space, thermal comfort metrics, and evaluation criteria.

2.1 Case Study: Industrial Building

Selecting an appropriate case study is critical in applied building energy research: the facility must contain sufficient typological variety to allow generalisation, while remaining specific enough for the findings to carry design relevance. The industrial manufacturing complex in Bagroda, Bhopal, Madhya Pradesh satisfies these requirements on three grounds. First, it comprises five distinct manufacturing shops: Machine Shop, Engine Shop, Weld Shop, Cab Trim Shop, and Chassis Assembly Shop, each with different processes, thermal loads, occupancy intensities, lighting power densities, creating an embedded comparative study within a single facility. Second, the complex was commissioned in 2021 and represents current Indian industrial construction practice. Third, Bhopal sits in the composite climate zone of India, characterised by hot, dry pre monsoon summers and warm, humid monsoon periods; a climate zone that includes a significant share of India's new manufacturing investment (Bureau of Indian Standards, 2016; Sharma, 2025). Findings from this facility therefore have direct transferability to a substantial and rapidly growing segment of the Indian industrial building stock.

The building under study is situated in Bagroda Industrial area, which is a suburb of the city of Bhopal. Madhya Pradesh, India 20 kilometres from the city centre. It is a 150 acre plot of land of which 55 acres has been built up. The factory is new and started operations in 2021.

The master plan of the Industrial facility can be seen in Figure 1. It is a manufacturing facility for small and large trucks and multiple shops are required for this process. These include a Machine Shop, Engine (Powertrain) Shop, Weld Shop, Paint Shop, Cab trim shop, Chassis Assembly Shop, Canteen, Administrative buildings, and various utility buildings. For this study, the main manufacturing industrial blocks have been considered.

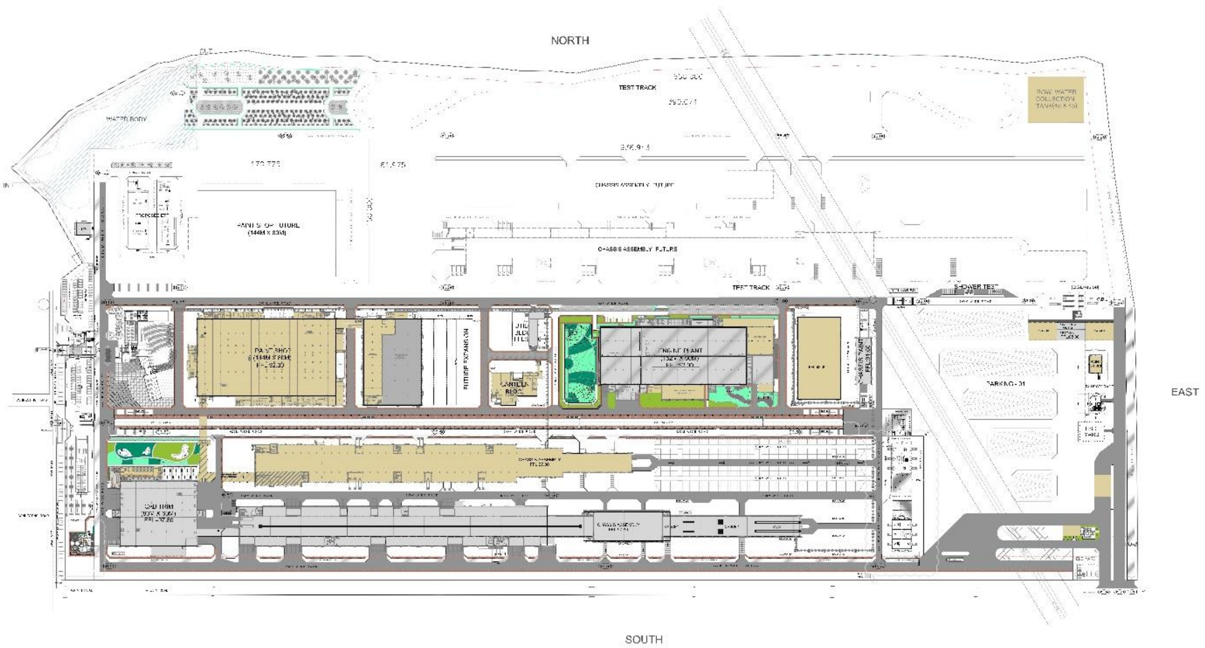

Figure 1. Master Plan of the Industrial Plant

The Paint Shop was excluded from this study. Its primary energy demand is dominated by process loads; spray booths, curing ovens, solvent extraction that are process specific, not building envelope driven, and outside the scope of building scale passive and low energy optimisation. Including it would require process engineering data and modelling approaches beyond the scope of this thesis.

The Cab Trim and the Assembly Shop are situated on the south of the site at the highest level of the site while the Machine Shop, Engine Plant and Weld Shop are situated towards the north of the Assembly and the Cab Trim Shop on the site, which is 6m lower.

The common construction methods include that the first 4m of the façade construction (seen from the ground) consists of cement blocks with cement plaster on the interior and the exterior. The construction after that till the roof is metal sheeting that continues over to the roof. This is discussed in the later sections.

Table 1. Summary of key characteristics of each building in the study

Name		**l**	**w**	**A**	**h**	**Roof**	**No. Bays**	**Daylighting**	**Cooling System**	**Process Types**
		[m]		**[m²]**	**[m]**					
Machine Shop		45	85	3825	15.5	North light bays	6	North vertical skylights, skylights	Evaporative Coolers	Automated Machining
Engine Shop		180	60	10800	12.5	Gable	1	skylights	AHU	Engine Assembly
Weld Shop		100	90	9000	15.5, 11.0	North light bays	6	North vertical skylights, skylights	Evaporative Coolers + HVLS Fans	Cabin Welding
Cab Trim Shop		90	60	5400	13.5	North light bays	4	North vertical skylights, skylights	Evaporative Coolers + HVLS Fans	Cabin Assembly
Chassis Assembly Shop	A	320	41	19000	13.5	North light bays	3	North vertical skylights, skylights	Evaporative Coolers + HVLS Fans	Truck Assembly
	B	48	21			North light bays	1	North vertical skylights, skylights		
	C	72	32			Gable	1	skylights		
	D	136	21			North light bays	1	North vertical skylights, skylights		

2.1.1 Machine Shop

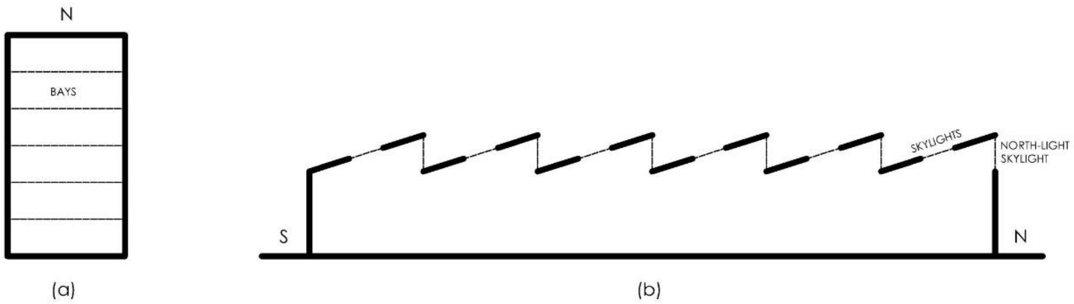

Figure 2. Schematic (a) Plan and (b) Section of the Machine Shop

The Machine Shop is a single-storey shed of 3,800 m², measuring 90 m wide and 45 m deep, with a ridge height of 15.5 m. The roof is divided into six parallel north light bays, each sloping downward to the south, with seven polycarbonate skylights (1 m × 3 m) distributed along the centreline of each bay and a vertical northlight at the northern edge of each bay. This building houses fully automated machining stations where workers are limited to inspection and inter station material transfer; it operates with evaporative cooling when required. Artificial lighting is provided only by LED high bay fittings used during night shifts, as the northlight system provides sufficient daylighting during the day.

2.1.2 Engine Shop

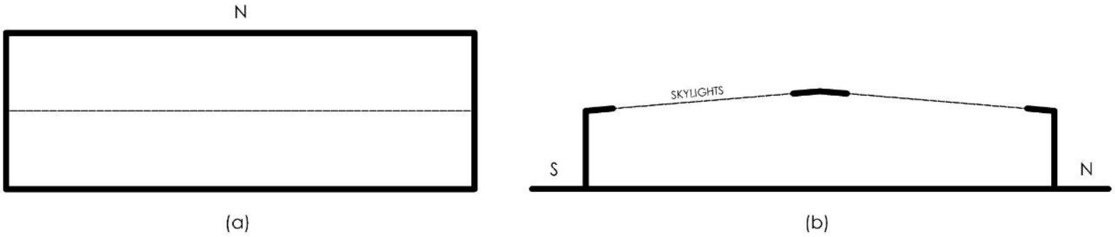

Figure 3. Schematic (a) Plan and (b) Section of the Engine Shop

The Engine Shop has a total floor area of 9,100 m², comprising a storage zone (60 m × 45 m) and a shop floor (60 m × 105 m), with the shop floor reaching 12.8 m at its highest point under a gable roof with an east west ridge. Material produced in the Machine Shop is brought to the storage area and assembled into complete engines at workstations across the shop floor. This is the only building with a conventional AHU based cooling system serving the shop floor; the storage zone is unconditioned. LED task lighting at each workstation is supplemented by mid bay and high bay LED fittings for general illumination, with skylights (25 m x 1 m) on the roof providing daytime natural light.

2.1.3 Weld Shop

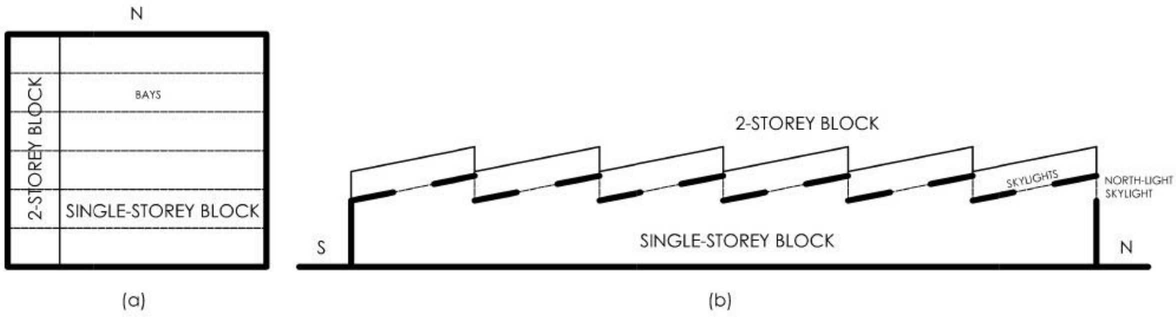

Figure 4. Schematic (a) Plan and (b) Section of the Weld Shop

The Weld Shop covers 9,000 m², measuring 90 m wide and 100 m deep, with a ridge height of 15.5 m at the topmost point. It can be divided into two areas: a single-story section (80 m x 90 m) and a 2-storey section (20 m x 90 m). These are both divided int six north light bays.

Sheet metal is formed and welded here into cabin frameworks, which are then transported to the mezzanine storage and then to the Paint Shop. Thermal comfort is provided by localised evaporative coolers mounted at roof level, with HVLS fans positioned in front of each supply diffuser to distribute cooled air across the working zone. Daylighting is delivered through 18 polycarbonate skylights (1 m x 3 m) per bay along the centreline and a vertical northlight at the head of each bay, and it has LED tube lights for task lighting, midbay and highbay LED lights for artificial lighting.

2.1.4 Cab Trim Shop

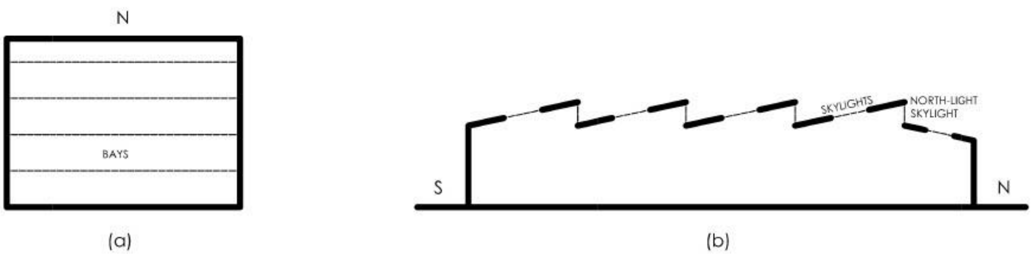

Figure 5. Schematic (a) Plan and (b) Section of the Cab Trim

The Cab Trim Shop is a single-storey building of 5,400 m², measuring 60 m wide and 80 m deep, reaching 13.5 m at its ridge. The roof follows a northlight bay configuration with the roof surface sloping southward; a separate smaller bay at the northern end slopes in the reverse direction, and all main bays are fitted with nine polycarbonate skylights (1 m x 3 m) and a vertical northlight. Painted truck cabins arrive from the Paint Shop and receive all interior fittings, before the completed cabin is transferred via an overhead bridge to the Chassis Assembly Shop. Localised evaporative coolers on the roof, paired with HVLS fans at each diffuser, provide cooling. The building also has LED mid bay, high bay, and task lighting.

2.1.5 Chassis Assembly Shop

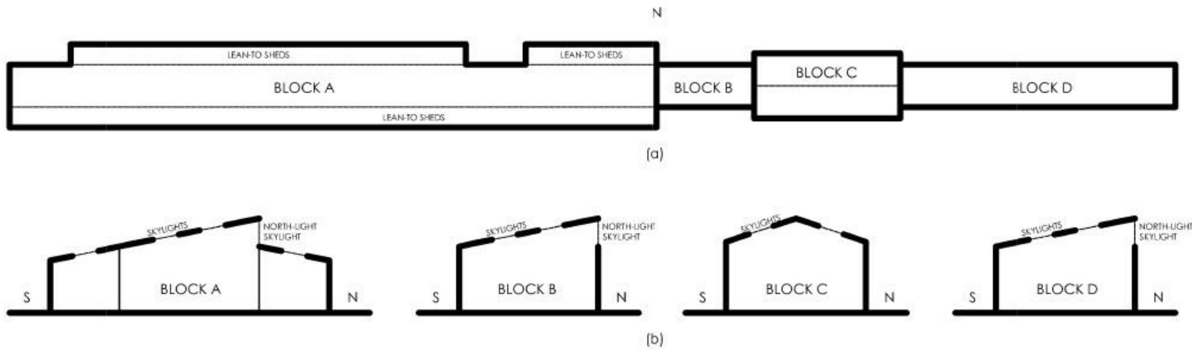

Figure 6. Schematic (a) Plan and (b) Section of the Assembly Shop

The Chassis Assembly Shop is the largest building on the site at 19,000 m² and is subdivided into four blocks from west to east for modelling purposes: Block A (320 m × 41 m, with 10 m lean-to sheds on both sides), Block B (48 m × 21 m), Block C (72 m × 32 m, gable roof), and Block D (136 m × 21 m). The central spine of Block A reaches 13.5 m, with the lean-to roofs at 9.5 m; Block C peaks at 13.5 m at the gable centreline. Chassis assembly proceeds linearly from west to east through Blocks A and B; Block C stores completed trucks awaiting testing, and Block D is used for pre delivery testing before trucks are driven to finished goods storage. Blocks A and B are served by large AHU based evaporative cooling systems with HVLS fans at each diffuser, while Blocks C and D have HVLS fans only; a total of 180 polycarbonate skylights (1 m x 3 m) across all blocks, together with vertical northlights on Blocks A, B, and D, provide daylighting across the full assembly line.

2.2 Data Collection

The parties involved in the design of this facility were contacted to get data of the factory. The architectural drawings, material specifications, were provided by the architects; the lighting drawings and specifications were provided by the lighting consultant; the electrical load (lighting and equipment) requirements were provided by the client along with the monthly annual energy consumption of each building for the year 2025.

A site visit was conducted in Feb 2026 to understand the functioning of the site and to take a closer look at the building, its construction, and to verify the drawings with the as built on site. More data was collected from facility managers; this included the manpower data of each building, this can be used to calculate the total occupancy as well as the occupancy schedules, equipment schedules and the lighting schedules for each building.

In 2025, the factory operated in two day shifts; some of the buildings were ready for use later in the year. The energy use data was gathered from the facility operation managers.

2.3 Energy Modelling and Simulation Workflows

2.3.1 Base Case Model Setup and Verification

Rhinoceros 3D was used to make the energy model of the industrial facility. Grasshopper along ClimateStudio was used to define the zones, relevant inputs and to run the energy simulations. The climate file used for the simulations was IND_MP_Bhopal-Bhoj.AP.426670_TMYx.2009-2023 EPW file (Climate.OneBuilding, 2023).

2.3.1.1 Formation of zones

Dividing the building into zones was challenging. The same zone has 2 different types of façade constructions, so the zone had to be divided into 2 vertical zones with an interior opening between the two for air mixing as seen in Figure 7 (a). The zones also had to be divided horizontally due to the large volume that one building comprises of and more internal openings had to be added to allow for air mixing as seen in Figure 7 (b).

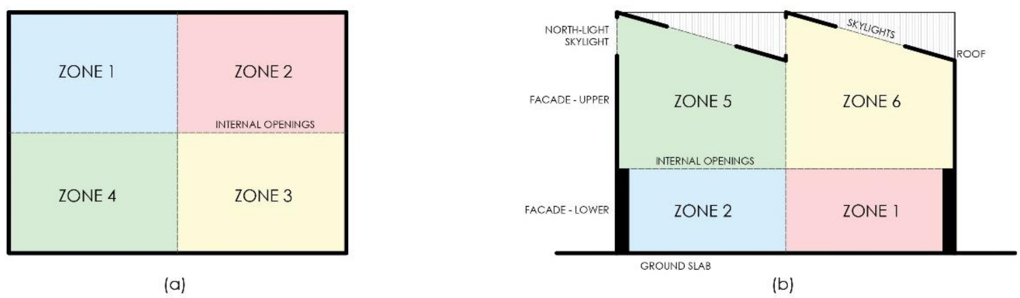

Figure 7. Diagrams showing zone separation in (a) plan and in (b) section.

2.3.1.2 Constructions and their thermal transmittance

The different construction types and their properties were retrieved from the architectural drawings. They can be seen in Table 2. These were the inputs used in grasshopper and ClimateStudio to run the simulations.

Table 2. Construction assembly types and U-values

Construction	Layers (Out to In)	Thickness	U - Value
	[-]	[m]	[W/(m².K)]
Roof	Metal Sheeting	0.015	0.19
	Glass Wool	0.2	
Façade - Upper	Metal Sheeting	0.015	3.841
Façade Lower	Plaster	0.015	2.31
	Brick Masonry	0.2	
	Plaster	0.015	
External Slab	Metal Sheeting	0.015	3.841
Partition	Plaster	0.015	0.4
	Aerated Cement Blocks	0.2	
	Plaster	0.015	
Ground Slab	Murum	0.2	1.659
	Hard-core metalling	0.2	
	PCC	0.075	
	Trimix Flooring	0.175	

2.3.1.3 People, Equipment, Lighting Density and their Schedules

The manpower data showed the factory shift timings. These can be seen in Table 3.

Table 3. Factory shifts schedule

Shift 1	Shift 2	Shift 3
0700 hrs - 1500 hrs	1600 hrs - 0000 hrs	0000 hrs - 0600 hrs

Metabolic rates were assigned per building based on the dominant task type at each manufacturing shop. Workers in the Machine Shop primarily perform light inspection and component transfer between automated machining stations, corresponding to a metabolic rate of 1.5 met. Workers in the Engine Shop, Weld Shop, Cab Trim Shop, and Chassis Assembly Shop perform sustained fabrication, welding, and assembly tasks, which are classified at 2.5 met consistent with ISO 8996 categories for medium to heavy assembly work involving whole body exertion (International Organization for Standardization (ISO), 2004).

Field studies used 2.0 met for machining workshop tasks and 2.5 met for assembly operations in Indian factory buildings and a metabolic rate of 2.2 met was measured in a rubber factory performing comparable physical manufacturing tasks (Kumar et al., 2020, 2021; Wang et al., 2018).

The sensitivity of comfort neutral temperature to metabolic rate is substantial, a change from 0.9 met to 1.5 met alone shifts the neutral operative temperature by approximately 3.2°C, a difference sufficient to move a worker from the acceptable to the unacceptable range under unchanged environmental conditions (Luo et al., 2018). The assignment of metabolic rates is therefore not a secondary modelling decision but one that directly determines which scenarios pass or fail the thermal comfort threshold.

The equipment loads were taken directly from the electrical load lists provided by the factory manager, these were the maximum loads that the buildings were designed to operate under. A calibration factor has been associated with each building and was used to calibrate the model with the onsite scenario as actual utilisation is lower than the design maximum. This data can be seen in Table 4.

Table 4. People and Equipment data per building

Name	Area	No. of people	People Density	Metabolic Rate	Real Equip. Load	Real Equip. Density	Correction Factor	Effective Equip. Load
	[m²]	[-]	[P/m²]	[met]	[W]	[W/m²]	[-]	[W/m²]
Machine Shop	3800	65	0.017	1.5	446.25	116.70	0.25	29.20
Engine Shop	9100	113	0.012	2.5	604.50	66.43	0.50	36.50
Weld Shop	9000	111	0.012	2.5	446.25	49.58	0.25	12.40
Cab Trim Shop	5400	86	0.016	2.5	330.75	61.25	0.25	15.30
Assembly Shop	19000	285	0.015	2.5	893.20	47.01	0.25	11.75

Annual simulations on each building were run under the assumption that they would operate under two shifts as this was the data available. Since the factory is capable of running three shifts, this might change the way the results are analysed.

The clothing value in the simulation is done using the ASHRAE comfort clothing model which automatically assigns clo values based on the temperature and the season (American Society of Heating, Refrigerating and Air-Conditioning Engineers, 2013).

Table 5 shows the lighting data for each building.

Table 5. Lighting and LPD data for each building

Name	Area	Type	Power	Quantity	Power	Total Power	Lighting Power Density
	[m²]		[W]	[-]	[W]	[W]	[W/m²]
Machine Shop	3800	Highbay	150	160	24000	24000	6.32
Engine Shop	9100	Highbay	280	100	28000	30376	3.34
		Midbay	12	63	756		
		Platform	30	54	1620		
Weld Shop	9000	Highbay	150	128	19200	28200	3.13
		Midbay	120	32	3840		
		Platform	40	129	5160		
Cab Trim Shop	5400	Highbay	100	100	10000	19440	3.60
		Midbay	80	23	1840		
		Platform	40	190	7600		
Chassis Assembly Shop	19000	Highbay	100	267	26700	47820	2.52
		Midbay	80	170	13600		
		Platform	40	188	7520		

2.3.1.4 Heating and Cooling Setpoints

All the buildings except the Engine Shop have evaporative coolers installed to improve thermal comfort. They are only used when internal temperatures exceed 35 °C. Evaporative cooler can cool the air by 5 °C - 8 °C. Table 6 shows the cooling setpoints for each building. A cooling availability schedule has been applied to the ventilation settings that cooling will only be available when the dry bulb temperatures exceed a certain number also shown in Table 6. Dry bulb temperatures are used as the control temperatures as this is what is used in the factory to manually switch on the evaporative coolers. The minimum supply air temperatures are higher than usual as this is an effort to simulate an evaporative cooler using an ideal air loads system.

Table 6. Building wise ventilation settings

Name	Cooling	Cooling Setpoint	Minimum Supply Air Temperature	Schedule
	Yes / No	°C	°C	
Machine Shop	Yes	35	32	DBT ≥ 34 °C
Engine Shop Floor	Yes	28	24	DBT ≥ 28 °C
Engine Shop Storage	No	-	-	-
Weld Shop	Yes	35	32	DBT ≥ 34 °C
Cab Trim Shop	Yes	35	32	DBT ≥ 34 °C
Chassis Assembly Shop	Yes	35	32	DBT ≥ 34 °C

The evaporative cooling systems installed across four of the five buildings are represented in the simulation using an ideal air loads system with a constrained minimum supply air temperature, rather than a physically detailed evaporative cooler module. This simplification is adopted for three reasons. First, the primary objective of the parametric study is comparative analysis across 385 scenarios per building rather than precise prediction of cooling energy; under these conditions, internal model consistency is more important than the thermodynamic details. Second, the parametric study varies envelope and operational parameters while holding the cooling system constant, so relative differences between scenarios remain valid even if absolute energy values vary. Third, the ideal air loads approach is widely used in multi building parametric simulation frameworks to reduce computational demand while preserving the ability to compare design measures (Dadras et al., 2025). The minimum supply air temperatures listed in Table 6 are set to reflect the achievable lower bound of an evaporative cooler operating in Bhopal's composite climate: a 5°C - 8°C depression of outdoor dry bulb temperature is achievable when the outdoor wet bulb depression is adequate, as is typical during the pre-monsoon summer when cooling demand is highest (Bishoyi & Sudhakar, 2017).

2.3.1.5 Infiltration

Infiltration is one of the most uncertain input parameters in building energy simulation, and this uncertainty is acknowledged as a limitation of the current model (Dadras et al., 2025). Infiltration in large span industrial buildings differs fundamentally from residential or commercial office buildings. Industrial sheds are designed for the continuous movement of raw materials, sub-assemblies, and finished goods, which requires large rolling shutters, loading bays, and vehicle access points to remain operational throughout the working shift. These openings create intermittent but high volume air exchange events that conventional infiltration modelling does not fully capture. Infiltration rates were estimated based on the operational characteristics of each building. A value of 0.4 ACH is assigned to buildings with frequent door operation and uninsulated metal sheet upper walls (Machine Shop, Weld Shop, Cab Trim Shop, and Chassis Assembly Shop). The Engine Shop is assigned 0.2 ACH given its fewer active operational openings. These values are estimates based on the observed operational characteristics of each building; no published benchmark specifically for large naturally ventilated Indian industrial sheds was identified. The infiltration rates are held constant across all 385 parametric scenarios within each building; relative comparisons between scenarios are therefore unaffected by the absolute infiltration value, though it influences the calibration of absolute energy totals against measured data. Table 7 shows the infiltration rates assigned to each building.

Table 7. Infiltration rates

Name	Infiltration [ACH]
Machine Shop	0.4
Engine Shop	0.2
Weld Shop	0.4
Cab Trim Shop	0.4
Chassis Assembly Shop	0.4

2.3.1.6 Windows, Rolling shutters and Skylights

The windows used in the buildings were single glazed units with Saint Gobain's ST 152 glass, the rolling shutters are manufactured by Gandhi automation and are made of aluminium and the polycarbonate sheets by Sabic (Gandhi Automation Pvt. Ltd., 2025; Sabic, 2013; Saint-Gobain Glass, 2025). The properties of these materials can be seen in Table 8 (Gandhi Automation Pvt. Ltd., 2025; Sabic, 2013; Saint-Gobain Glass, 2025).

Table 8. Thermal properties of the openings used.

Opening Type	Material	Type	U - value [W/(m².K)]	SHGC [-]
Window	Glass	Single	5.5	0.44
Skylight	Polycarbonate	Single	3.2	0.47
Rolling Shutter	Steel	-	5	0.01

2.3.1.7 Internal Windows

As shown in Figure 7, the building had to be broken into multiple zones. To ensure there was air mixing among these zones an opening had to be created. Table 9 shows the properties of the internal window.

Table 9. Internal window properties

Material	U - value	SHGC	Operable Area	Discharge Coefficient	Vent Control
	[W/(m².K)]	[-]	[-]	[-]	[-]
AirWall	0	0.99	1	1	Constant

Operable area = 1 means that the entire area of the window will be able to transfer air, discharge coefficient = 1 is the ease at which mixing will occur and vent control = constant aids constant mixing of air.

2.4 Parametric studies

2.4.1 Lighting efficiency

As shown in Table 5, the installed LPD values for the case study buildings range from 2.52 W/m² to 6.32 W/m². These values are significantly lower than both the ASHRAE 90.1-2016 limit of 9.70 W/m² and the ECBC 2017 baseline of 12.0 W/m², confirming that the as built design already represents a high efficiency lighting specification (American Society of Heating, Refrigerating and Air-Conditioning Engineers, 2016; Bureau of Energy Efficiency (BEE), 2017). In comparison, the IGBC Green Factory Building Rating Version 2.0 requires the installed LPD to be at least 10% below the ECBC 2017 baseline (The Indian Green Building Council (IGBC), 2025).

The lighting power density in each building was tested that the minimum compliance value of 9.70 W/m² to test increase in energy requirements from the base scenario.

2.4.2 Factory operation scheduling

The factory operates two shifts per day. As documented in the data collection phase, the actual operating pattern in 2025 consisted of two consecutive daytime shifts as seen in Table 10. However, the factory infrastructure is designed to support a third shift, this raises the question of whether reorganising the two active shifts so that one of them occupies this night shift would have a meaningful effect on the building's energy use. This parametric variation is therefore included to test whether the timing of occupancy, independent of any change to the building envelope or systems, can be used as an energy saving measure.

During a daytime shift, the buildings are naturally daylit through the skylights on the north light girders that are present on each building. This means that artificial lighting can be substantially reduced or switched off during occupied daytime hours. A night shift, by contrast, takes place in complete darkness and requires the full artificial lighting load to be active for the entire shift duration. At the same time, the ambient dry bulb temperature in Bhopal (Climate Zone 1B, composite climate zone) is highest in the afternoon and lowest in the early morning hours before sunrise (Bureau of Indian Standards, 2016; Climate.OneBuilding, 2023). Operating the factory at night should reduce cooling loads as the temperatures are lower.

Two shift configurations were therefore defined for simulation, as shown in Table 10. Scenario A represents the current operational pattern with both shifts occurring during daytime and evening hours. Scenario B replaces the second shift with the night shift, maintaining the same total number of occupied hours and worker counts per building.

Table 10. Tested shift schedules

Sr. No.	Shift 1	Shift 2	Shift 3
A	0700 hrs - 1500 hrs	1600 hrs - 0000 hrs	not applicable
B	0700 hrs - 1500 hrs	not applicable	0000 hrs - 0600 hrs

2.4.3 Insulation on roof and walls

The roof is the dominant pathway for solar heat gain into single-storey industrial buildings in hot climates. In composite and hot dry Indian climate zones, the roof accounts for 50% - 60% of the total cooling load of a building (Rawat & Singh, 2022). For large span industrial sheds with thin metal sheet roofs, the thermal mass of the roof is negligible, making it highly responsive to solar radiation during the day and to sky radiative cooling at night. The existing buildings are insulated and provide significant resistance to daytime heat conduction. Removing this insulation is tested as the counterfactual representing older or lower cost industrial sheds in India. Adding insulation to the uninsulated upper metal sheet walls is tested simultaneously as a complementary envelope measure, since the upper wall in all five buildings is an uninsulated single sheet metal façade.

A two level test is used for the roof rather than multiple, because the primary design decision is binary: whether having insulation itself is beneficial or not. Gentle et al. (2011) performed Systematic EnergyPlus simulations across 18 parameter combinations showing that beyond a moderate insulation level ($R \approx 1.6$ m²K/W), further increases in R-value show strongly diminishing returns on cooling load reduction, and can actively reduce the benefit of night sky radiative cooling in buildings with significant internal heat loads as insulation that prevents daytime heat ingress equally prevents the rejection of internally generated heat at night (Gentle et al., 2011). The existing insulation (200 mm glass wool, $R \approx 5.0$ m²K/W) already exceeds this threshold, making the comparison between insulated and uninsulated an important test for the buildings.

Table 11. Insulation thickness tested

Sr. No.	Insulation thickness [mm]	
	A	B
Roof Wall	0	200

While roof insulation consistently reduces daytime heat conduction and therefore lowers cooling energy demand, its effect on thermal comfort is more nuanced. An experimental comparison of insulation, reflective coating, and PCM strategies on real scale test chambers in Raipur, the same climate classification as Bhopal, the results showed that an insulated roof reduced the peak ceiling temperature by 9.6 °C - 12.3 °C relative to an uninsulated reference room during extreme summer conditions, but also increased the minimum nighttime ceiling temperature by 2.7 °C (a -9.3% change relative to the reference), while a cool roof reduced the minimum ceiling temperature by 1.3 °C (Verma et al., 2026).

2.4.4 Reflective roof coatings

Cool roofs are defined as roof surfaces with high solar reflectance that reduce the absorption of shortwave solar radiation, thereby lowering roof surface temperature and the heat conducted into the building below. In composite and warm humid Indian climate zones, cool roof application has been shown to reduce building energy use by 14% - 26% and average roof surface temperature by up to 1.4°C, with the largest benefits accruing during the pre-monsoon summer months when solar radiation intensity is highest (Rawat & Singh, 2022). Factories, shopping centres, and airport terminals have been identified as the highest priority targets for cool roof application because the roof to floor ratio in these building types amplifies the energy benefit of albedo change relative to the investment cost (Gentle et al., 2011). Table 12 shows the roof absorptance ratios.

Table 12. Roof Absorptance Ratios

Roof Absorptance Ratios		
A	B	C
0.7	0.5	0.2

Three roof reflectance values are tested in this study: 0.7, 0.5 and 0.2. These levels span the practical range of albedo values achievable without structural modification and are consistent with the albedo ranges examined across Indian and tropical cool roof studies (Rawat & Singh, 2022; Zingre et al., 2015). Gentle at al. (2011) showed that by using EnergyPlus simulations, peak cooling load reductions of 2.5 - 3.5 times are achievable by reducing solar absorptance from 0.8 to 0.2 regardless of the insulation R-value, confirming that albedo is the dominant roof material parameter in warm climate buildings (Gentle et al., 2011). An experiment in the composite climate of India, where a reflective coating with solar reflectance of 0.95 achieved an annual energy conservation ratio of 7.2% - 21.9% depending on building operating hours, comparable to the insulated roof scenario (Verma et al., 2026).

The interaction between solar reflectance and roof insulation is a critical consideration in interpreting the combined results of these two parametric measures. At high albedo (solar absorptance ≈ 0.2), the additional energy benefit of increasing R-value above a moderate threshold is negligible, while at low albedo (solar absorptance ≈ 0.8) a high R-value is essential to manage daytime heat gain (Gentle et al., 2011). This suggests that the two roof parameters are dependent. In the present study, all three albedo levels are simulated in combination with both insulated and uninsulated roof conditions, allowing this interaction to be characterised for each building typology. Furthermore, Verma et al. (2026) note that Reflective coatings, unlike insulation, also reduce minimum nighttime ceiling temperature by approximately 1.3°C, which may improve overnight comfort recovery in buildings where internal process heat loads accumulate during the working shift (Verma et al., 2026).

2.4.5 High efficiency windows and skylights

The base case buildings use single glazed glass windows and single skin polycarbonate sheet skylights. The thermal properties of these openings, as obtained from the architectural drawings and material specifications, are shown in Table 8.

Given that the roofs and facades of these buildings receive significant solar irradiation in Bhopal, improving the thermal and solar performance of windows and skylights represents a potentially worthwhile energy intervention. Higher performance glazing can reduce heat gain through two mechanisms: a lower U-value reduces conductive heat transfer driven by the temperature difference between indoors and outdoors, while a lower SHGC reduces the solar radiation that passes through the glazing as heat into the building. Three progressively higher performing configurations are therefore defined for both windows and skylights, as detailed in Table 13.

Table 13. Properties of windows and skylights

Type	Name	Material	Type	U - value [W/(m².K)]	SHGC [-]
Window	Window01	Glass	Single	5.4	0.44
	Window02		Double	1.1	0.6
	Window03			1.1	0.4
	Window04			0.7	0.3
Skylight	Skylight01	Polycarbonate	Single	3.56	0.66
	Skylight02			1.8	0.55
	Skylight03			1.2	0.4
	Skylight04			0.9	0.3

2.4.6 Final simulation combinations

Figure 8 shows all the combinations tested in the parametric simulation workflow for one building. The same combinations have been tested for the others. The lighting power density has only been applied to one case (red line) to test the effect when it is increased. This results in 385 simulations for each building and a total of 1925 simulations conducted (2x2x2x3x4x4 = 384 combinations + 1 higher LPD case = 385 combinations per building).

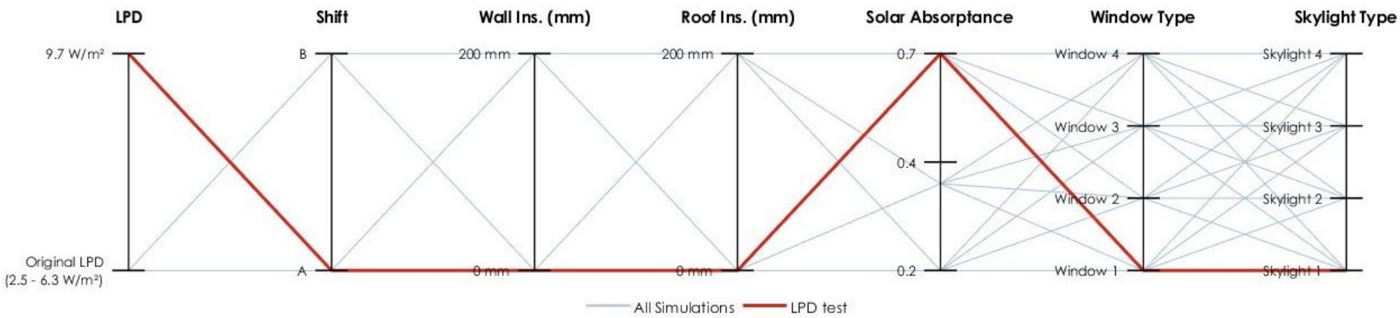

Figure 8. Parallel Coordinate plot showing all the parametric combinations.

2.5 Thermal Comfort Metrics

Thermal comfort in industrial buildings in warm climates presents a fundamentally different challenge from the sedentary office environments for which most international standards are developed. Workers in manufacturing environments perform physical tasks at elevated metabolic rates of 2.0 met - 2.5 met, are exposed to process heat, and rely primarily on natural ventilation, evaporative cooling, and fan assisted air movement rather than conventional air conditioning (International Organization for Standardization (ISO), 2004, p. 8; Kumar et al., 2020, 2021).

Three comfort models are used in this study across three airspeed levels and two acceptability bands, yielding eighteen distinct evaluation metrics in total. The first model is the Indian Model for Adaptive Comfort for naturally ventilated buildings (IMAC-NV), it is the nationally recognised office-level adaptive baseline (Manu et al., 2016). The second is IMAC-W, an adaptation of IMAC-NV for industrial workers at elevated activity levels (Kumar et al., 2020, 2021; Wang et al., 2018). The third is the Standard Effective Temperature (SET), a physiologically independent benchmark that integrates airspeed through a two node thermoregulatory model (Gagge et al., 1972, 1986).

2.5.1 Indian Model for Adaptive Comfort (IMAC)

The IMAC was proposed based on a nationwide field study of 6,330 thermal comfort responses collected from 16 office buildings across five Indian climate zones; Warm Humid (Chennai), Hot Dry (Ahmedabad), Composite (Delhi), Moderate (Bengaluru), and Cold (Shimla) (Manu et al., 2016). The study followed Class II measurement protocols derived from the ASHRAE RP-884 framework, recording indoor air temperature, globe temperature, relative humidity, and air velocity at the workstation level simultaneously with thermal sensation and acceptability votes (Manu et al., 2016).

The central finding was that occupants in naturally ventilated (NV) and mixed mode (MM) Indian office buildings are significantly more thermally adaptive than international standards such as ASHRAE 55 and EN 16798-1 would predict (Manu et al., 2016). The PMV model was found to consistently over predict the sensation on the warmer end of the scale for all building types, with the discrepancy ranging from 0.5 to 1.0 sensation vote at indoor operative temperatures between 22°C and 30°C (Manu et al., 2016). Adaptive thermal comfort models for NV and MM buildings were derived using the Griffiths Method, with a Griffiths constant of 0.16 for both building types resulting in the IMAC model for NV using the following equation (Manu et al., 2016):

$$T_{neutral} = 0.54 \times T_{running\ mean} + 12.83 \quad (1)$$

Where $T_{neutral}$ is the indoor operative temperature at neutral sensation, $T_{running\ mean}$ is the 30 day outdoor mean air temperature.

The 80% and 90% thermal acceptability bands are ±4.1°C and ±2.4°C around the neutral temperature, respectively (Manu et al., 2016).

The 30 day outdoor running mean temperature is calculated using the exponentially weighted formula:

$$T_{rm(tomorrow)} = 0.8 \times T_{rm(yesterday)} + 0.2 \times T_{m(today)} \quad (2)$$

Where Tm(today) is the daily mean outdoor air temperature .

This formulation was adopted in the present study using hourly outdoor dry bulb temperature data from the Bhopal-Bhoj EPW climate file.

The IMAC model was subsequently incorporated into the National Building Code of India (2016) as the nationally applicable comfort standard for naturally ventilated and mixed mode commercial buildings (Bureau of Indian Standards, 2016). The model was also extended into a residential version (IMAC-R), based on yearlong field surveys in 294 residences across eight cities in the five Indian climate zones, yielding 2,179 validated responses (Rawal et al., 2022). The IMAC-R study confirmed that Indian occupants exhibit greater thermal adaptability than both IMAC-commercial and international standards predict, with a neutral temperature up to 2.1°C warmer than IMAC-NV at comparable outdoor temperatures (Rawal et al., 2022). This further supports the appropriateness of the IMAC framework for Indian buildings where occupants are acclimatised to the local climate. (Manu et al., 2016; Rawal et al., 2022).

2.5.2 Metabolic Rates and the Limitation of IMAC in Industrial Contexts

The IMAC model was developed from data collected in office environments at low metabolic rates (1.0 met - 1.4 met) (Manu et al., 2016). This presents a direct limitation for the present study: workers in manufacturing facilities operate at substantially higher metabolic rates, typically 2.0 met - 2.5 met for assembly and fabrication tasks (ISO 8996) which significantly changes the thermal neutral temperature and the acceptability of air movement (International Organization for Standardization (ISO), 2004; Luo et al., 2018).

Metabolic rate is one of the six fundamental parameters in the Fanger heat balance model and the most difficult to estimate accurately in field conditions (Luo et al., 2018). Changing metabolic rate from 0.9 met to 1.5 met alone produces a variation of approximately 3.2°C in the thermally neutral temperature, a difference large enough to shift a worker from acceptable to unacceptable comfort conditions within the same physical environment (Luo et al., 2018). In industrial buildings where different shops involve different task intensities, the assignment of metabolic rates therefore has a direct and significant effect on the comfort outcomes reported (Luo et al., 2018).

The ASHRAE 55 adaptive comfort model is formally restricted to metabolic rates of 1.0 met - 1.3 met (sedentary to light work) and is therefore not directly applicable to any of these buildings (American Society of Heating, Refrigerating and Air-Conditioning Engineers, 2013).

2.5.3 IMAC-W: Extension of IMAC to Industrial Buildings

Having established both the IMAC framework and the metabolic rate conditions of the study buildings, it is necessary to verify whether IMAC remains valid at elevated activity levels and to define the airspeed adjusted acceptability bands appropriate for factory workers. For the purposes of this study, the IMAC model as extended to workshop environments is referred to as IMAC-W. IMAC-W applies the IMAC-NV neutral temperature equation with airspeed adjusted acceptability bands derived from field studies in Indian industrial workshop buildings (Kumar et al., 2020, 2021). It should be noted that IMAC-W is not a formally standardised model; it represents an operational adaptation of IMAC-NV using empirically validated airspeed corrections, applied here as an analytical framework for comparative assessment.

A field study in a naturally ventilated engineering workshop building at NIT Jalandhar collected 1,332 thermal comfort responses from students engaged in machining and fabrication tasks at approximately 2.0 met across two seasons (Kumar et al., 2020). A high correlation was found between outdoor running mean temperature and indoor comfort temperature (Kumar et al., 2020):

$$T_c = 0.81 \times T_{rm} + 6.03 \quad (3)$$

Where T_c is the comfort temperature, T_{rm} is the 30 day running mean. This adaptive relationship has a steeper slope than both the IMAC-NV model and ASHRAE 55, indicating that occupants engaged in industrial activities are more sensitive to outdoor temperature fluctuations than sedentary office workers (Kumar et al., 2020). Subjects accepted indoor airspeeds up to 2.0 m/s during autumn, and an approximately 2.3°C increase in neutral globe temperature was observed when airspeed increased from 0.5 m/s to 1.0 m/s (Kumar et al., 2020). This is directly consistent with the finding from a broader field study of 2,610 responses in naturally ventilated buildings in Jaipur, which demonstrated that subjects are comfortable up to 35°C at airspeeds of 0.5 m/s - 1.5 m/s, compared to 32°C under still air conditions (Kumar et al., 2016).

A complementary field study in a naturally ventilated transformer manufacturing factory in Jaipur, the same composite climate as Bhopal collected 1,276 responses from 325 workers across summer and winter seasons (Kumar et al., 2021). A factory specific adaptive comfort equation was proposed (Kumar et al., 2021):

$$T_c = 0.61 \times T_{pm} + 14.67 \quad (4)$$

Where T_c is the comfort temperature, T_{pm} is the prevailing monthly mean air temperature. This gave a slope steeper than both IMAC-NV and ASHRAE 55, further confirming that factory workers are more sensitive to outdoor conditions than office occupants (Kumar et al., 2021). Probit analysis showed over 80% of workers reported comfort across a wide indoor temperature range of 24.2°C - 34.6°C (Kumar et al., 2021). Fan use was observed to shift the comfort temperature upward by approximately 4°C during summer; consistent with, but slightly higher than, the 2.3°C shift derived from workshop data (Kumar et al., 2021). The AS1 airspeed threshold used in this study (+2.3°C) therefore represents the more conservative lower bound of these two empirical estimates (Kumar et al., 2020, 2021).

A comparable field investigation in a rubber manufacturing factory in Zibo, China, further corroborates the adaptive framework in industrial contexts (Wang et al., 2018). A field investigation in a rubber factory in Zibo, China collected thermal comfort responses from 40 workers performing inspection and material handling tasks at a weighted metabolic rate of 2.2 met (comparable to the assembly line activities in the present study) under naturally ventilated summer conditions (Wang et al., 2018). The observed neutral temperature derived from actual thermal sensation votes was 21.2°C, compared to a PMV predicted neutral temperature of 18.3°C; this discrepancy of 2.9°C is consistent with the Indian workshop findings and confirms that the PMV model systematically overestimates thermal sensation at elevated metabolic rates in manufacturing environments (Wang et al., 2018). The proposed adaptive model yielded a 90% acceptable operative temperature range of 23.2°C - 32.2°C and an 80% range of 26.3°C - 33.3°C (Wang et al., 2018). Importantly, the slope of the adaptive model derived for rubber factory workers was steeper than all comparable office and residential models, indicating that factory workers adapt more rapidly to outdoor temperature fluctuations than sedentary occupants in Indian workshop buildings (Kumar et al., 2020, 2021).

Collectively, these studies confirm two key points for the present work. First, the IMAC adaptive framework, linking indoor comfort temperature to outdoor running mean temperature extends to industrial workshop buildings in the Indian composite climate (Kumar et al., 2020, 2021). Second, elevated airspeed from fan operation shifts the upper comfort threshold meaningfully upward, and this shift must be explicitly included when evaluating thermal comfort in these buildings (Kumar et al., 2020, 2021).

The 90% acceptability upper limit under elevated airspeed in the present study is therefore derived by applying the IMAC-NV model upper band limit (±2.4°C at 90%) and increasing the upper threshold by 2.3°C in the AS1 (first elevated airspeed, ~0.6 m/s - 0.8 m/s) and by 3.3°C for the AS2 (second elevated airspeed, >1.0 m/s) condition (International Organization for Standardization (ISO), 2005; Kumar et al., 2020). The 80% band applies the same increments to the IMAC-NV 80% upper limit.

The physical mechanism by which these airspeeds are delivered in the study buildings is by using High Volume Low Speed (HVLS) fans is described in the following section.

2.5.4 HVLS Fans and the Physical Basis for Airspeed Thresholds

The airspeed thresholds defined in IMAC-W are physically delivered in the study buildings through High Volume Low Speed (HVLS) fans, installed alongside evaporative cooling diffusers in the Assembly Shop, Weld Shop, and Cab Trim Shop, and as standalone circulation devices in areas without cooling. HVLS fans are large diameter, low speed ceiling mounted fans that generate a broad, uniform column of descending air across the floor area (Ecoair, 2024a, 2024b). A single HVLS fan distributes air across up to 28,000 sq. ft of floor area, replacing multiple wall mounted or pedestal fans at significantly lower operating cost and with reduced draft risk (Ecoair, 2024a).

The comfort benefit of HVLS fans in industrial buildings derives primarily from two mechanisms: enhanced convective heat loss from the skin surface and increased evaporative cooling through sweat evaporation (Zhai et al., 2015). Self-controlled air movement has been shown to maintain thermal comfort, perceived air quality, and acceptability at temperatures up to 26°C during moderate exercise (2 met - 6 met) compared to a 20°C no fan baseline, with preferred air speeds increasing from approximately 0.2 m/s at 2 MET to 2.3 m/s at 6 met (Zhai et al., 2015)A preferred temperature paradigm confirmed that subjects exercising at 3.0 met - 4.5 met preferred temperatures 1.6°C - 2.8°C higher with self-controlled fan than without, and that all subjects were satisfied with their chosen thermal environment (Zhai et al., 2020). These findings are directly relevant to the factory context, where workers performing assembly and welding tasks at 2.0 met - 2.5 met use elevated airspeed as a primary adaptive mechanism (Zhai et al., 2015, 2020).

Table 14. established airspeed bands for thermal comfort analysis

Band	Airspeed Range	Comfort Shift
AS1	0.6 - 0.8	+2.3° C shift to upper limit
AS2	>1.0	+3.3°C shift to upper limit

These airspeeds correspond to typical HVLS fan delivery at occupant level in large volume industrial sheds (Ecoair, 2024a). The no airspeed condition was not evaluated as the primary scenario because workers in these buildings would invariably switch on fans before reaching severe thermal discomfort, making the still air condition an impractical lower bound for operational assessment. This is supported by the logistic regression analysis which found that 80% of fans were activated when indoor globe temperature reached 32°C, providing a direct behavioural basis for the AS1 threshold (Kumar et al., 2021).

This worker centred preference for elevated airspeed as a comfort management strategy is not limited to the Indian context. A study of garment factory workers in Bangladesh examined sustainable cooling strategies for a similarly challenging occupational environment: hot humid climate, high occupancy density, and physical manufacturing tasks at elevated metabolic rates (Smallcombe et al., 2025). The study found that passive cooling combined with elevated airspeed was preferred by workers over mechanical air conditioning, and that standard heat stress indices such as WBGT significantly under predicted comfort acceptability when airspeed was present (Smallcombe et al., 2025). This pattern where air movement elevates the effective upper comfort threshold beyond what static heat balance or heat stress models predict is now consistently observed across multiple manufacturing typologies and climate zones in South and Southeast Asia (Kumar et al., 2020, 2021; Smallcombe et al., 2025; Wang et al., 2018). These findings strengthen the methodological decision to apply airspeed adjusted IMAC-W thresholds.

2.5.5 Standard Effective Temperature

The Standard Effective Temperature (SET) is a single number index that integrates all six classical thermal comfort parameters; air temperature, mean radiant temperature, relative humidity, air velocity, clothing insulation, and metabolic rate through a two node physiological model of human thermoregulation (Gagge et al., 1972). Unlike the PMV model, which is based on a steady state heat balance, SET uses a model of skin temperature and skin wettedness to represent the body's actual physiological response (Gagge et al., 1972). SET is defined as the operative temperature in a standard environment (50% RH, 0.1 m/s air velocity, 0.6 clo, 1.0 met) that would produce the same skin temperature and skin wettedness as the actual environment under the actual clothing and activity conditions (Gagge et al., 1986).

SET is included in this study as a complementary metric for two reasons. First, it explicitly accounts for the physiological effect of elevated airspeed through its skin wettedness model, making it theoretically more sensitive to the cooling benefit of HVLS fan operation than the band based IMAC-W approach. Second, it is entirely independent of the adaptive comfort framework and therefore provides a verification check on IMAC-W results.

In this study, SET is computed directly by ClimateStudio via EnergyPlus (U.S. Department of Energy (DOE), 2025). The acceptability thresholds for SET are 80% and 90% acceptability, consistent with the IMAC bands, allowing direct comparison across metrics.

2.5.6 The final metrics

Each metric is defined by the combination of the thermal model (IMAC-NV, IMAC-W or SET), acceptability band (80% or 90%), and airspeed assumption (AS0, AS1, or AS2). Each metric is reported as the percentage of occupied hours during which the indoor operative temperature exceeds the corresponding upper acceptability threshold. Higher values indicate worse thermal conditions. These metrics can be seen in Table 15.

Table 15. Thermal Comfort Metrics

Airspeed	90% BAND			80% BAND		
	IMAC	IMAC-W	SET	IMAC	IMAC-W	SET
AS0	$IMAC_{90}$	$IMAC\text{-}W_{90}$	SET_{90}	$IMAC_{80}$	$IMAC\text{-}W_{80}$	SET_{80}
AS1	$IMAC_{90\_AS1}$	$IMAC\text{-}W_{90\_AS1}$	SET_{90_AS1}	$IMAC_{80\_AS1}$	$IMAC\text{-}W_{80\_AS1}$	SET_{80_AS1}
AS2	$IMAC_{90\_AS2}$	$IMAC\text{-}W_{90\_AS2}$	SET_{90_AS2}	$IMAC_{80\_AS2}$	$IMAC\text{-}W_{80\_AS2}$	SET_{80_AS2}

2.6 Evaluation criteria

The study evaluates design strategies across two simultaneously tracked performance objectives: energy efficiency, measured as annual Energy Use Intensity (EUI) in kWh/m² of conditioned floor area, and thermal comfort, measured as the percentage of occupied hours during which the indoor air temperature exceeds the IMAC-W upper acceptability threshold under specified airspeed conditions. These two objectives are not assumed to be aligned; identifying whether low energy scenarios also tend to be low discomfort, or whether design strategies create trade-offs between the two outcomes, is one of the central analytical questions of the study.

Energy Use Intensity (EUI) is defined in this study as the sum of annual site energy consumption from three categories; lighting energy, equipment energy, and cooling energy divided by the conditioned floor area of each building (kWh/m²/year). Process energy beyond the thermal contribution of equipment to the space is excluded, as it is not accessible through building-scale envelope or operational interventions. This definition is applied consistently across all five buildings and all parametric scenarios.

EUI is used as the primary energy metric rather than total annual energy consumption because it normalises for building size and enables direct comparison across the five buildings. EUI also aligns with the metric used by the IGBC Green Factory Building rating system for benchmarking industrial buildings in India, providing a direct connection between simulation results and certification relevant performance thresholds (The Indian Green Building Council (IGBC), 2025). Both the 80% and 90% acceptability bands are reported to distinguish between buildings.

EUI comparisons across buildings must be interpreted with caution, as the five buildings differ substantially in process-generated internal loads. The Machine Shop's equipment density (36 W/m²) is approximately 3x that of the Chassis Assembly Shop (11 W/m²), meaning that envelope-driven strategies will have a proportionally smaller impact on EUI in process-dominated buildings. Cross-building EUI comparisons are therefore used to characterise typological diversity rather than to rank building efficiency.

All 385 scenarios per building are evaluated on both metrics individually and then simultaneously. Design measures are compared by computing the mean change in EUI and the mean change in thermal comfort attributable to each measure, averaged across all combinations of the remaining parameters. This approach, consistent with a screening methodology, isolates the independent contribution of each variable and reveals whether any measure reduces energy while simultaneously worsening comfort, or vice versa. Scenarios are also visualised as scatter plots of EUI versus thermal comfort to identify how the two objectives are related across all scenarios for each building.

3 RESULTS AND DISCUSSION

3.1 Validation of the Base Case energy model

Table 16 compares simulated annual electricity consumption against measured billing data for each building for the year 2025.

Three of the five buildings fall within an 8% deviation from metered annual energy consumption. For a design-phase comparative parametric study, where the primary objective is the relative ranking of scenarios rather than absolute energy prediction, this level of agreement is considered acceptable; note that calibration in such contexts prioritises internal model consistency over strict statistical convergence to billing data (Chong et al., 2021). The Weld Shop shows the largest discrepancy at 27.6%, which can be justified due to a partial year operations, the Weld Shop commenced two shift operations partway through 2025, while the simulation assumes a full 52 week operating year at two shift occupancy. When scaled to the proportion of the year in which the building was fully operational, the effective deviation falls within the same range as the other four buildings.

Table 16. Actual vs Simulated annual energy per building.

Name	Actual Scenario	Simulated Scenario	Percentage Difference
	MWh	MWh	%
Machine Shop	630.4	719.4	12.4
Engine Shop	2366.7	2407.9	1.7
Weld Shop	517.1	714.1	27.6
Cab Trim Shop	493.8	525.3	6.0
Chassis Assembly Shop	1385.8	1340.1	3.4

The objective of the simulation is not to predict absolute annual energy totals with high precision, but to produce consistent relative rankings across the 385 scenarios per building; a goal for which internal model consistency matters more than absolute accuracy (Dadras et al., 2025). The calibrated base cases are therefore accepted as valid starting points for the parametric study.

3.2 Global Energy Performance across all scenarios

This section presents the energy performance results across all parametric scenarios for the five buildings. The analysis proceeds in two steps: first, the overall EUI range spanned by the 385 scenarios per building is characterised to identify the boundaries of possible performance by isolating the base case, best case, and worst case scenarios. Second, all the scenarios are plotted on one graph in increasing order of EUI to understand the energy trends.

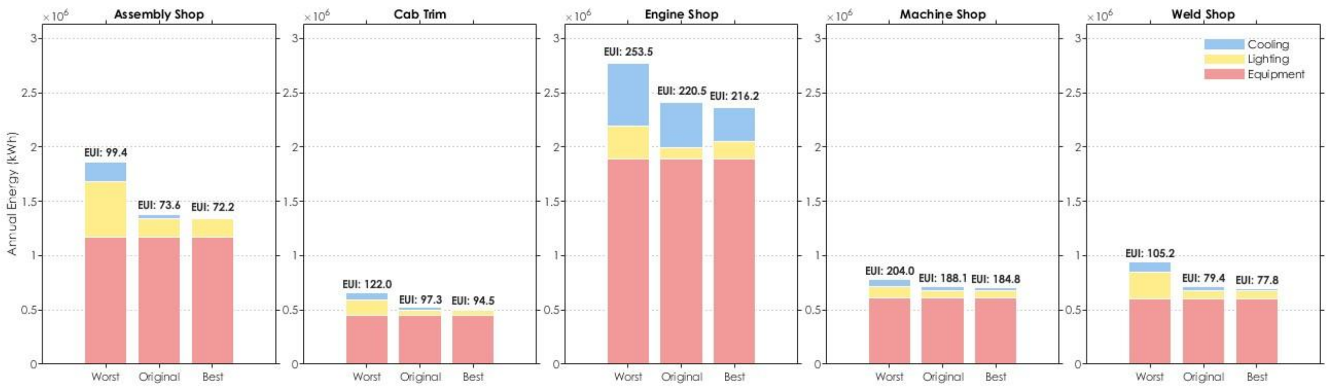

Figure 9. Energy Breakdown of 3 scenarios in each building

Figure 9 shows the energy breakdown of 3 cases: the original case, the worst case and the best case for each building. Each scenario shows the total annual energy use breakdown into cooling energy, lighting energy and equipment energy.

Closer inspection of the ranked EUI curve from Figure 10 reveals that the 385 scenarios do not form a smooth gradient but instead cluster into five discrete performance bands, consistent across all five buildings, these can be seen in Table 17.

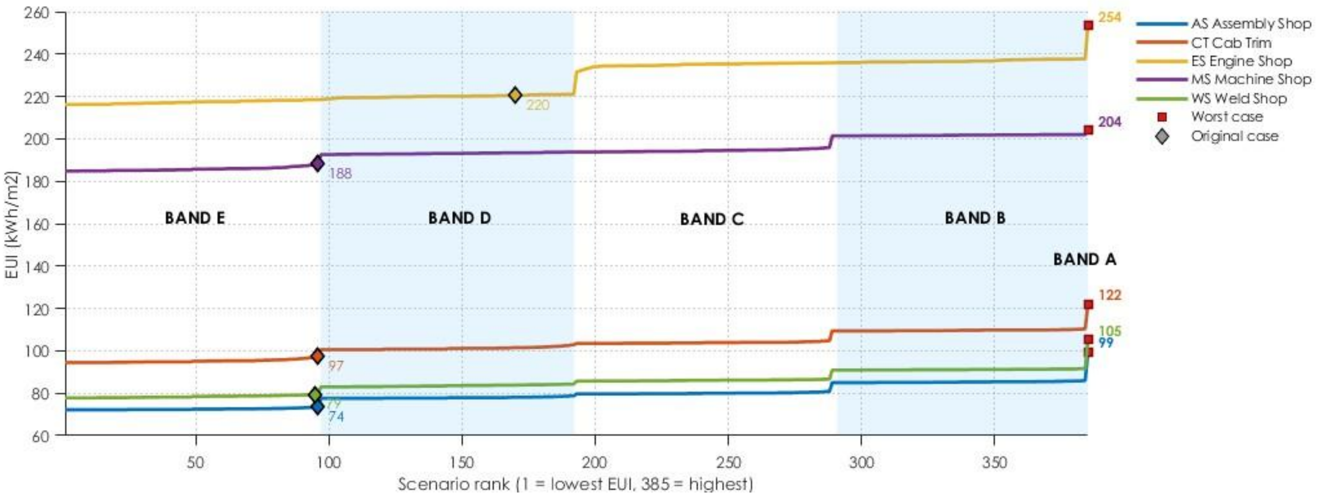

Figure 10. Building-wise EUI of all iterations in increasing order

Table 17. Visible bands based on EUI

Band	LPD	Shift	Insulation		Windows	Skylights
			Roof	Wall		
A	9.7	A	No		Inconsequential	
B	Original	B	No		Inconsequential	
C	Original	B	Yes		Inconsequential	
D	Original	A	No		Inconsequential	
E	Original	A	Yes		Inconsequential	

- Band A - The highest EUI band contains a single scenario combining the code level LPD (9.7 W/m²), Shift A (day schedule), and no roof insulation, this is the worst case.
- Band B - The next band groups scenarios with the original LPD, Shift B (day night shift) and no roof insulation.
- Band C - This band adds roof insulation to the previous band combination.
- Band D – Here the band consists of the original LPD, Shift A (two day shifts), and no roof insulation.
- Band E - the lowest band combines the original LPD with Shift A and roof insulation. This step structure confirms that LPD, shift schedule, and roof insulation are the three parameters that define EUI tier, while the remaining variables (wall insulation, window type, skylight type, solar absorptance) cause the within band variation. The practical implication is immediate: a designer who gets these three decisions right will place a building in the lowest EUI tier regardless of the other choices made.

This banding structure is the central finding of the energy analysis, it demonstrates that three design parameters; Lighting Power Density (LPD), shift schedule, and roof insulation together determine the EUI tier in which a building operates, while the remaining four variables (wall insulation, window type, skylight specification, and solar absorptance) produce a within band scatter without shifting a building between tiers.

The Engine Shop deviates from this five band pattern. Here, the dominant structure in the EUI distribution is a binary split between insulated and uninsulated scenarios, without the clear LPD and shift driven stratification seen in others. This is explained by the Engine Shop's typological distinction; it is the only building served by a conventional AHU system with a 28°C cooling setpoint. The cooling system's continuous mechanical demand suppresses the relative contribution of lighting and shift effects, making roof heat gain the single dominant variable. This confirms that the three parameter EUI hierarchy is a property of naturally ventilated and evaporatively cooled industrial buildings in this climate, and that mechanically cooled buildings require a separate analysis framework.

Looking at Figure 11 and Table 18, across all the buildings, there is ~ 2% improvement from the original case. This shows the importance of having a low LPD as well as installing roof insulation. In other cases where the LPD is high and there is no roof insulation there can be savings ~ 25%.

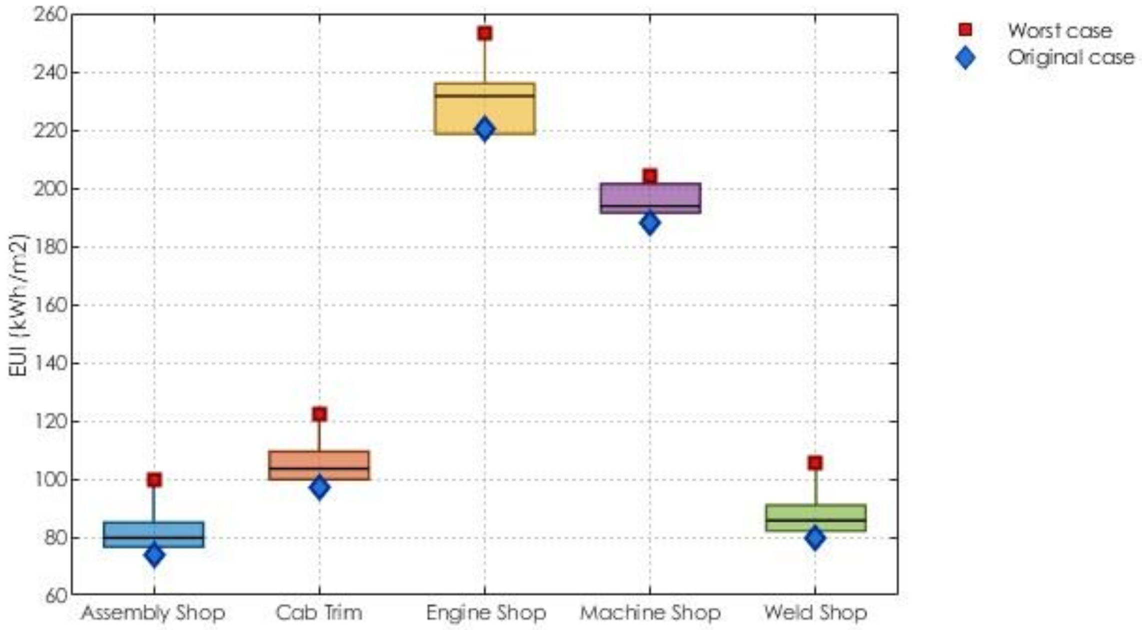

Figure 11. EUI distribution across all parametric scenarios (boxplots)

Table 18. Building wise potential energy savings

Name	Original Case	Worst Case	Best Case	Best Case improvement w.r.t	
				Original	Worst
Assembly Shop	74	99	72	2%	27%
Cab Trim Shop	97	122	95	3%	23%
Weld Shop	79	105	78	2%	26%
Engine Shop	220	253	216	2%	15%
Machine Shop	188	204	185	2%	10%

The machine shop shows a lower improvement ratio as this is the building that does not have a cooling load as the occupancy is very minimal, so equipment and lighting loads dominate. Equipment loads cannot be changed so LPD becomes the primary factor to reduce energy use.

The Engine shop also shows a lower potential for energy savings as this has a hight equipment load as well as it a lower cooling setpoint than other buildings, hence it requires a larger amount of energy for cooling. It is to note that the setpoints are the same in all cases, so these values are still comparable.

Figure 11 also shows the improvement ranges for each building and the position of the original case. It shows that the Engine shop has the highest variation while all the other buildings have a tighter range of improvement. In all five buildings, the original scenario lies at or near the lower bound of the EUI distribution.

The original design already lies close to the lower EUI side of the distribution in all buildings, meaning the as built design is already relatively efficient. However, the worst case comparisons still reveal substantial consequences if poor lighting and roofing decisions are made.

3.3 Influence of design strategies on Energy Use

After identifying the broad EUI bands, the next step is to isolate which individual design measures are responsible for the largest changes in energy use.

Figure 12 breaks down the mean EUI change attributable to each design measure across all buildings. The ranking confirms the banding structure identified in the previous section.

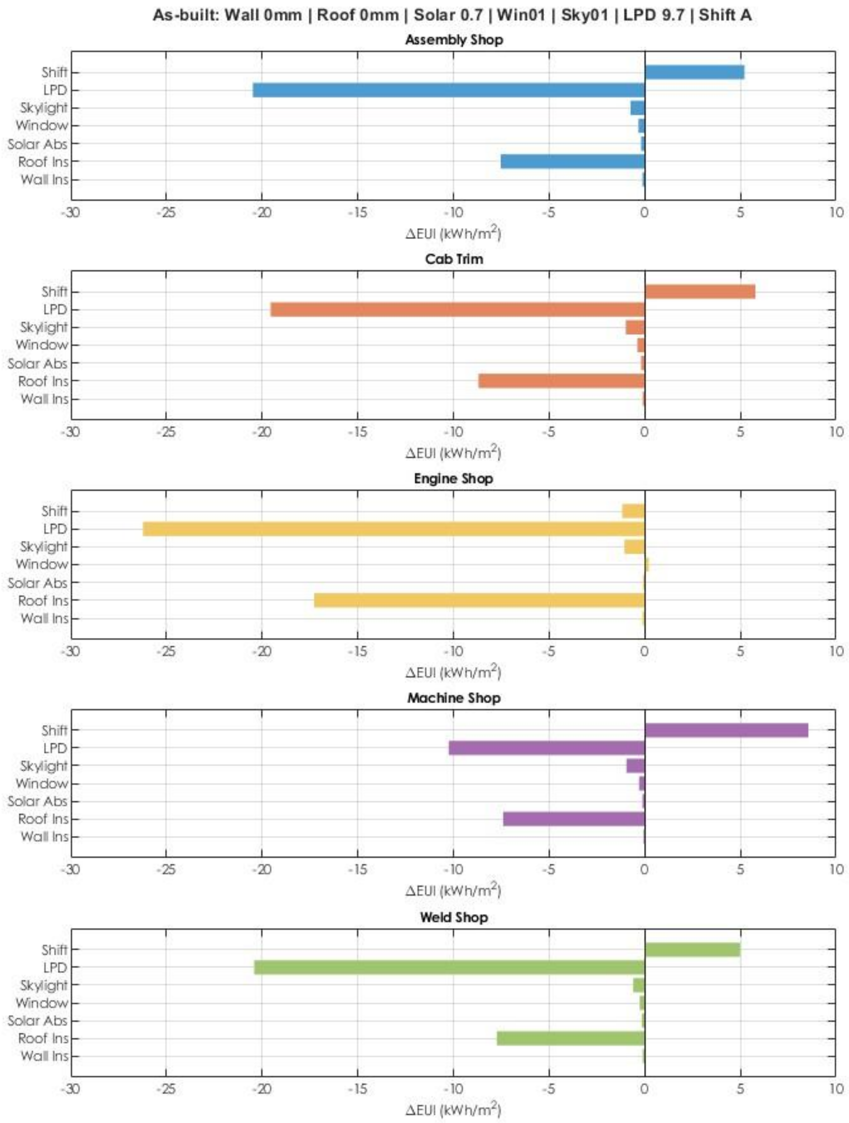

Figure 12. Mean ΔEUI per measure

Lighting Power Density is the primary factor in reducing energy use. As in factories the lighting loads are large and it adds electricity use as well as internal gains to the building, this number makes a significant difference in energy use at ~20 kWh/m^2. This effect operates through two mechanisms; direct electricity consumption and additional cooling load required from the waste heat generated by higher wattage light fittings. The finding is consistent across all five buildings and confirms the conclusion that internal heat gains are the primary driver of thermal and energy performance in Indian manufacturing buildings where HVAC is limited or absent (Dadras et al., 2025; Rawat & Singh, 2022).

The next measure which makes the most impact is having roof insulation; this reduces the EUI on average by ~10 kWh/m^2. These measures are consistent across all the buildings. This is consistent with the literature: in Indian composite and hot dry climate buildings, the heat gain via the roof accounts for 50% - 60% of the total cooling load (Rawat & Singh, 2022).

Shift scheduling is the third ranked measure, reducing EUI by approximately 6 kWh/m^2 when both shifts are operated during daytime hours (Shift A) versus a day night split (Shift B). The mechanism is a trade-off between lighting and cooling loads. The night shift eliminates the daylighting contribution of the skylights, requiring full artificial lighting throughout the second shift, while simultaneously reducing cooling loads as outdoor temperatures drop. In four of the five buildings, the lighting load increase outweighs the cooling saving. The Engine Shop is the exception: here the two effects approximately cancel, yielding a net shift effect of <1 kWh/m^2. This again reflects the Engine Shop's higher mechanical cooling load.

Skylight upgrade produces a mean EUI reduction of approximately 2 kWh/m^2, divided roughly equally across the three upgraded levels (02, 03, 04), yielding less than 1 kWh/m^2 per specification level. This modest return is explained by the relatively small, glazed area of the skylights relative to the total roof area in these buildings.

Wall insulation, solar absorptance (cool roof coating), and window specification do not produce statistically meaningful EUI changes across the parametric range tested. The result is consistent with the study which demonstrated that in buildings where internal heat gains are large relative to envelope gains, reducing roof solar absorptance reduces peak cooling load significantly but has a smaller effect on total annual energy use because the building's energy balance is dominated by internal loads for a larger share of the occupied year (Gentle et al., 2011). In the present buildings, equipment and process loads constitute the largest single component of total energy use in all five shops; under these conditions, cool roof coatings are more valuable as a thermal comfort intervention than as an energy-saving measure.

3.4 Thermal Comfort Metrics Evaluation

Industrial environments, especially those relying on natural ventilation and elevated air speeds challenge standard comfort models, it is essential to determine how different metrics compare.

The eighteen metrics are evaluated pairwise to establish the degree of agreement between the three comfort models. This analysis evaluates the correlation between the Indian Model for Adaptive Comfort (IMAC), Indian Model for Adaptive Comfort Workshop Model (IMAC-W) and the Standard Effective Temperature (SET). Table 19 and Table 20 report Pearson correlation coefficients for three comparisons; IMAC-W versus IMAC, IMAC-W versus SET, and IMAC versus SET at each of the three airspeed levels and both acceptability bands, computed across all 385 parametric scenarios per building. Establishing the degree to which these metrics align is a prerequisite for interpreting the comfort outcomes of the design measures tested.

Table 19. Thermal comfort metric correlation - 90% band.

Name	IMAC-W$_{90}$ x IMAC$_{90}$			IMAC-W$_{90}$ x SET$_{90}$			IMAC$_{90}$ x SET$_{90}$		
	AS0	**AS1**	**AS2**	**AS0**	**AS1**	**AS2**	**AS0**	**AS1**	**AS2**
Assembly Shop	0.51	0.99	0.95	0.29	0.08	0.11	0.37	0.10	0.06
Cab Trim Shop	0.72	0.98	0.99	0.67	0.14	0.09	0.61	0.13	0.11
Weld Shop	0.96	0.99	0.98	0.32	0.04	0.03	0.32	0.01	0.02
Engine Shop	0.93	0.96	0.96	0.79	0.95	0.89	0.95	0.85	0.76
Machine Shop	0.79	0.94	0.92	0.00	0.31	0.46	0.00	0.29	0.66
Average	**0.78**	**0.97**	**0.96**	**0.41**	**0.30**	**0.31**	**0.45**	**0.28**	**0.32**

Table 20. Thermal comfort metric correlation - 80% band.

Name	IMAC-W$_{80}$ x IMAC$_{80}$			IMAC-W$_{80}$ x SET$_{80}$			IMAC$_{80}$ x SET$_{80}$		
	AS0	**AS1**	**AS2**	**AS0**	**AS1**	**AS2**	**AS0**	**AS1**	**AS2**
Assembly Shop	0.99	0.93	0.90	0.10	0.15	0.11	0.11	0.11	0.10
Cab Trim Shop	0.93	0.98	0.96	0.19	0.08	0.15	0.30	0.07	0.07
Weld Shop	0.99	0.99	0.98	0.12	0.05	0.16	0.03	0.02	0.12
Engine Shop	0.98	0.98	0.97	0.97	0.82	0.65	0.92	0.74	0.75
Machine Shop	0.91	0.92	0.97	0.00	0.18	0.12	0.00	0.24	0.11
Average	**0.96**	**0.96**	**0.96**	**0.28**	**0.26**	**0.24**	**0.27**	**0.24**	**0.23**

At AS1 airspeed, IMAC-W and IMAC show a linear agreement across all five buildings, confirming that IMAC-W does not fundamentally reorder the scenario rankings relative to the adaptive standard. At AS0, the correlation is weaker in three buildings, indicating that the relative ordering of scenarios is sensitive to the airspeed assumption. This finding consistent with the thermal sensitivity analysis which showed that small changes in boundary conditions produce large reordering effects near comfort thresholds (Zhai et al., 2015).

The correlation coefficients across all building types as seen in Table 19 and Table 20 reveal a linear relationship ($r > 0.96$) between IMAC-W and IMAC. This suggests that for these facility types and climate conditions, IMAC-W provides a highly reliable proxy for adaptive comfort. Conversely, the correlation between IMAC and IMAC-W with SET is significantly weaker, indicating that SET is sensitive to different physiological or environmental variables than the adaptive models. This lack of correlation is pronounced once elevated air speeds are integrated into the simulation, confirming that SET serves as an independent benchmark.

The correlation between the adaptive metrics (IMAC-W, IMAC) and SET is weaker across all buildings and airspeed levels. The weak average correlation does not indicate that SET is insensitive to the design scenarios but rather reflects a fundamental difference in how the two models respond. The adaptive models assign comfort based on the occupant's acclimatisation to the outdoor running mean temperature; a building's thermal environment is relative to what the occupant expects (de Dear, 1998; Gagge et al., 1986; Manu et al., 2016). SET evaluates the physiological strain imposed on the body at the actual indoor conditions, independent of expectations. In buildings dominated by internal process heat loads where indoor temperatures remain consistently elevated throughout the year, the two models produce different rankings as they are asking different questions about the same environment.

Given the IMAC-W × IMAC-NV correlation at AS1, results focus on IMAC-W$_{90_AS1}$ as the primary comfort metric. The deviation of SET, particularly its insensitivity to the air speed measures highlights that it functions as a more conservative metric, reflecting the high activity levels and thermal loads in industrial manufacturing facilities.

3.5 Thermal comfort response by measure

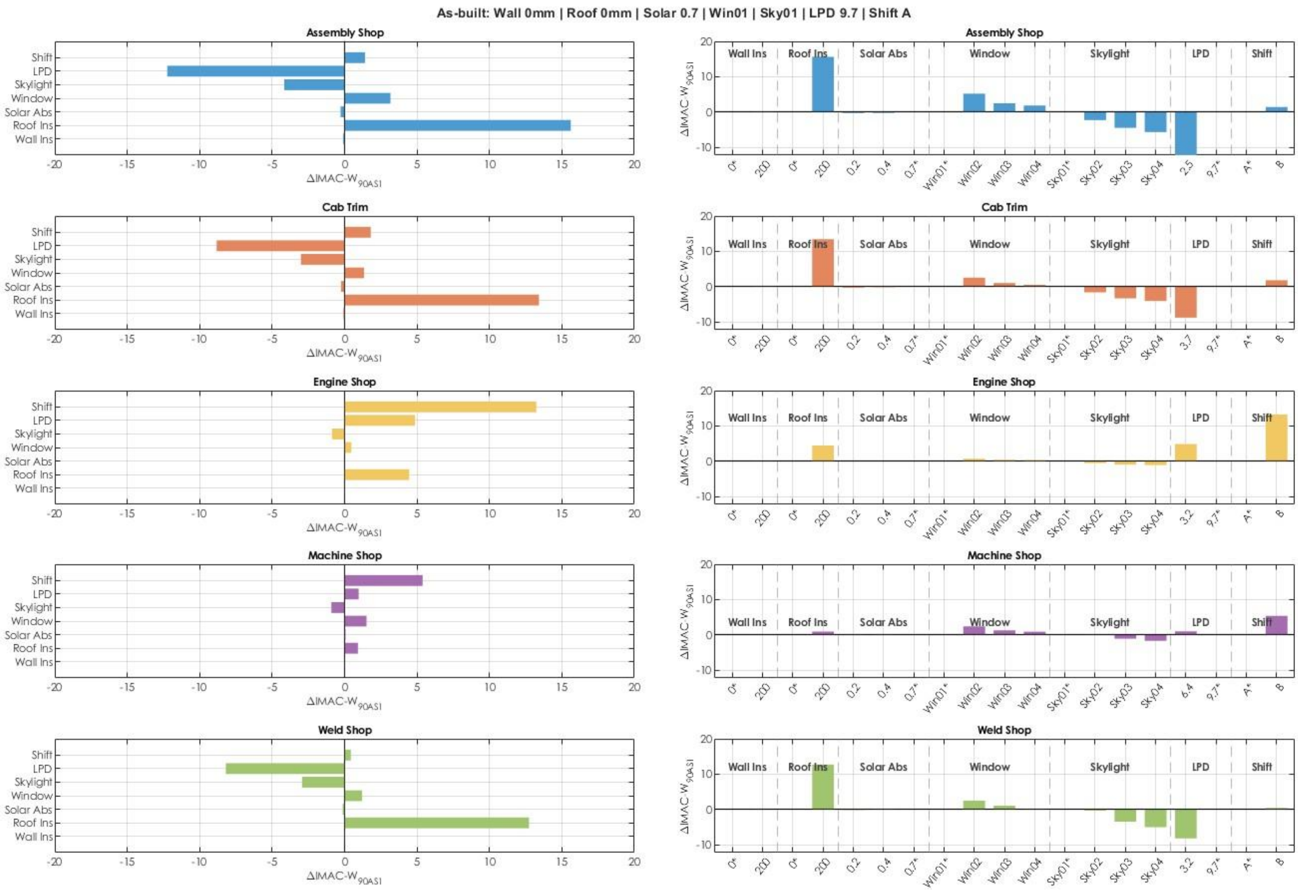

Figure 13. Mean ΔIMAC-W$_{90AS1}$ per measure and per level of each measure

The thermal comfort metric IMAC-W$_{90_AS1}$ is used for this analysis. This represents the most conservative of the operationally realistic comfort conditions; the minimum fan intervention that workers would routinely apply before experiencing significant discomfort ensuring that any improvements here are robust across the remaining higher airspeed and lower acceptability threshold metrics.

Figure 14 shows the mean change in IMAC-W$_{90_AS1}$ attributable to each design measure. Unlike the EUI response, comfort does not resolve into a consistent pattern across the five buildings. Instead, two distinct response typologies emerge:

- Load Sensitive Response: In these buildings, lighting generates a significant share of the total internal heat load relative to the process equipment load, so LPD reduction simultaneously reduces peak indoor temperatures and discomfort hours.
- Load Resistant Response: In these buildings, the impact of LPD is weakened. This indicates that process related heat gains or building volume effects dominate the internal climate, rendering LPD control a secondary strategy for comfort management.

The thermal comfort response to roof insulation is a counterintuitive finding in this analysis. In the Cab Trim Shop and Weld Shop, adding roof insulation increases discomfort hours. This appears to contradict the energy result (insulation reduces EUI) but can be justified: insulation that prevents solar heat gain during the day equally prevents the rejection of process generated heat to the environment. This has been identified experimentally, where a 2.7°C increase in minimum nighttime ceiling temperature was measured in an insulated test chamber relative to an uninsulated reference under the same composite climate conditions (Verma et al., 2026). In buildings with high continuous process loads, the thermal mass of the building envelope is insufficient to absorb and emit this heat, so it accumulates across the first shift and persists into the second shift period (Gentle et al., 2011; Rawat & Singh, 2022). The practical implication is that roof insulation alone is not a sufficient comfort strategy for high process load buildings, it must be paired with adequate night ventilation or heat exhaust capacity to realise its comfort benefit.

Shift schedule B (day night split) consistently degrades thermal comfort. Despite the lower ambient outdoor temperatures during the night shift, the accumulated process heat from the first shift cannot be dissipated, and the building's thermal mass has insufficient capacity to recover to comfortable temperatures before workers arrive for the second shift. This finding has direct operational relevance: if the facility expands to three shift operation, the night shift workers in process heat dominated buildings will face systematically worse comfort conditions than the first-shift workers.

The wall insulation does not change the thermal comfort at all. This confirms that for these large volume industrial sheds, the wall envelope is irrelevant compared to the roof and the internal processes.

3.6 Comfort vs energy trade-offs by building

The previous sections treated energy and comfort separately, but real design decisions must balance both outcomes at once. The EUI vs IMAC-W plots with pareto fronts are therefore used to determine whether low energy scenarios also deliver acceptable comfort, or whether the two goals diverge.

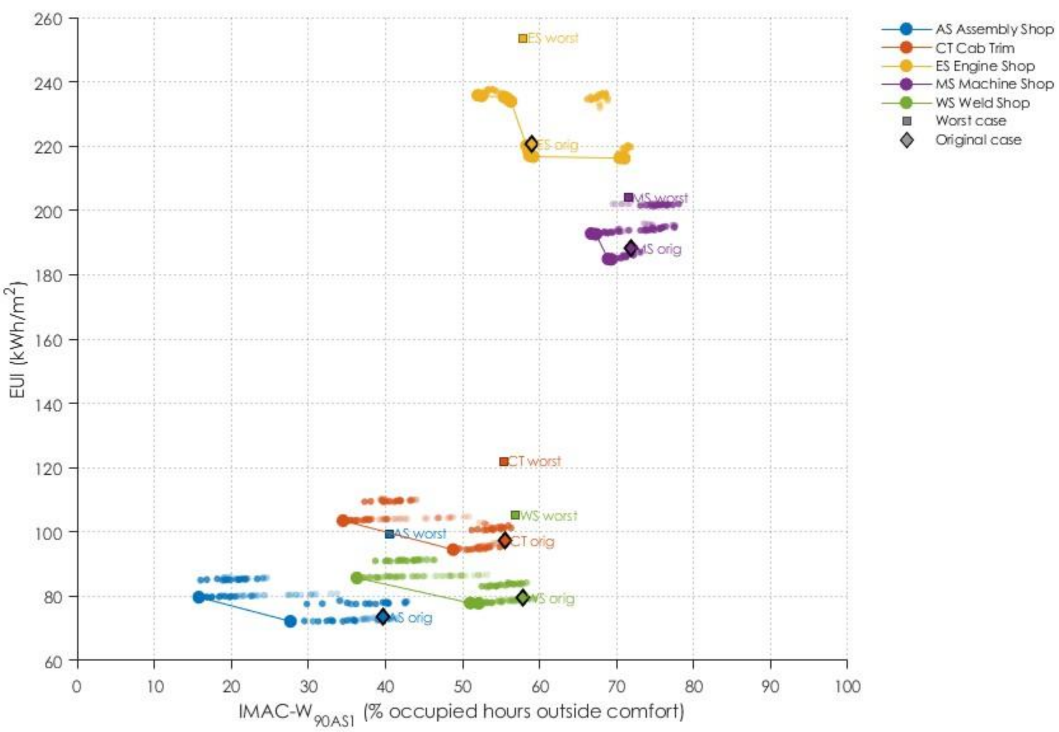

Figure 14. EUI x Thermal Comfort plot (IMAC-W$_{90AS1}$) with pareto fronts for all buildings

Table 21. Percentage of overheating occupied hours (IMAC-W_{90_AS1}) and EUI per building for original case, worst case and best case.

Name	EUI Ranking	EUI	90% Band			80% Band		
			No Airspeed	Airspeed 1	Airspeed 2	No Airspeed	Airspeed 1	Airspeed 2
Assembly Shop	**Original**	73.6	65.6	39.8	21.4	49.1	8.3	0.7
	Worst	99.4	66.8	40.5	25.6	49.0	13.8	2.8
	Best	72.2	62.7	30.6	6.2	45.0	0.7	0.0
Cab Trim Shop	**Original**	97.3	70.8	55.6	43.4	60.4	33.4	16.1
	Worst	122.0	71.7	55.3	44.3	71.7	35.3	21.1
	Best	94.5	68.4	50.5	30.1	57.0	13.5	1.3
Weld Shop	**Original**	79.4	70.5	57.8	46.4	62.1	37.0	19.3
	Worst	105.2	71.7	56.9	46.6	61.5	37.6	24.1
	Best	77.8	66.9	52.1	34.6	57.1	16.8	1.2
Engine Shop	**Original**	220.5	84.7	59.0	54.4	61.6	50.1	42.9
	Worst	253.5	84.4	57.9	52.6	60.4	48.9	41.3
	Best	216.2	87.8	71.0	66.8	73.4	61.0	47.7
Machine Shop	**Original**	188.1	85.3	71.8	66.6	75.9	62.0	51.9
	Worst	204.0	84.7	71.5	66.1	75.5	61.5	51.5
	Best	184.8	85.1	69.3	62.1	73.5	53.7	36.0

HVLS fan operation, provides the largest absolute reduction in discomfort hours of any intervention analysed.

As seen in Table 21, moving from AS0 to AS1 reduces IMAC-W_{90} from 65.6% to 39.8% of occupied hours in the Assembly Shop, from 70.5% to 57.8% in the Weld Shop, and from 70.8% to 55.6% in the Cab Trim Shop. These reductions are larger than the total comfort improvement achievable through any combination of passive envelope changes. This finding confirms that self-controlled elevated airspeed is the primary adaptive mechanism available to workers at 2 met - 3 met in warm climates, and provides simulation based evidence that the HVLS fan infrastructure already installed in three of the five buildings is the most impactful comfort measure (Zhai et al., 2015, 2020).

Chassis Assembly Shop: This building shows the clearest alignment between energy and comfort objectives. The best case scenario improves on both scales relative to the original case. The Pareto front is populated by scenarios combining low LPD, Shift A, and roof insulation which are the three parameters that drive energy performance. This arises because LPD reduction simultaneously reduces lighting electricity consumption and the internal heat load that elevates indoor temperatures during the shift. A designer can navigate toward the best quadrant by making the same three decisions that minimise EUI, without any comfort penalty.

Cab Trim Shop: A similar but less pronounced alignment is observed. The best case EUI scenario also achieves the lowest $IMAC_{90\_AS1}$.

Weld Shop: The pattern here introduces the first significant trade off. Roof insulation improves EUI but worsens $IMAC_{90\_AS1}$, meaning that the best EUI scenarios are not the best comfort scenarios. The Pareto plot shows a negative slope; a lower EUI is associated with higher discomfort. This trade off arises specifically because of the Weld Shop's process loads, and the insulated roof prevents heat rejection. The practical design recommendation is to specify insulation with a night ventilation strategy. The energy benefit of insulation is substantial, but it requires a parallel heat exhaust pathway to deliver its comfort benefit.

Engine Shop: The Engine Shop lies almost entirely in the high discomfort quadrant across all 385 scenarios. EUI varies significantly but $IMAC_{90\_AS1}$ remains above 57.9% in all the scenarios. This exists because the Engine Shop's 28°C AHU setpoint means that roof insulation, the main energy saver, reduces the frequency of AHU activation; a side effect of fewer cooling cycles is slightly higher operative temperatures during non-conditioned periods. This is the clearest case in the study of a building where passive optimisation is insufficient: the Engine Shop's comfort problem requires a lower cooling setpoint.

Machine Shop: The Machine Shop shows the smallest spread in both EUI and $IMAC_{90\_AS1}$, reflecting its unique characteristics: automated machining with very low occupancy density and a high equipment load. Passive envelope changes move the building's energy performance marginally, and comfort remains persistently poor under all scenarios. However, since the Machine Shop does not require constant occupancy and only regular checking, thermal comfort could be disregarded. If thermal comfort must be reduced, installing an AHU with mechanical cooling will be required.

Taken together, the five buildings establish a spectrum of design challenge. At one end, the Assembly Shop and Cab Trim Shop offer genuine co benefits: the same decisions that minimise energy also improve comfort, and passive optimisation is a viable strategy. The Weld Shop presents a resolvable trade off: insulation and night ventilation together achieve both objectives that insulation alone cannot. At the other end, the Engine Shop and Machine Shop require interventions beyond the passive envelope.

4 CONCLUSIONS

This study characterised the energy use intensity and thermal comfort environment of five manufacturing buildings at a truck production facility in Bhopal, Madhya Pradesh, through calibrated whole building energy simulation and an 18 metric adaptive and physiological thermal comfort evaluation across 1,925 parametric scenarios.

The five buildings span a baseline EUI range from 74 kWh/m² to 220 kWh/m². This range reflects three distinct typological drivers: building volume per unit floor area (larger, higher buildings dissipate heat more effectively), cooling system type (evaporative versus mechanical), and the ratio of process equipment load to floor area. The Engine Shop and Machine Shop, which combine high equipment densities with mechanically cooled environments, are at the energy intensive end of the spectrum. Looking at thermal comfort; in the primary metric, the Machine Shop (71.8% discomfort hours) and Engine Shop (59.0%) are the worst performers due to their high equipment loads. The Assembly Shop achieves the lowest discomfort (39.8%) despite its large floor area, confirming that cooling system design and HVLS fan coverage are stronger predictors of comfort outcomes than building size or EUI.

LPD is the single most influential strategy for both energy and comfort in naturally ventilated and evaporatively cooled buildings. It reduces EUI by ~20 kWh/m² and, in load sensitive buildings, reduces discomfort hours through the reduction in internal heat gain. Roof insulation reduces EUI by ~10 kWh/m² consistently but produces a thermal comfort penalty in process heat dominated buildings by preventing heat rejection (Verma et al., 2026). HVLS fan operation (moving from AS0 to AS1 airspeed) produces the largest absolute reduction in discomfort hours; up to 25.8 percentage points in the Assembly Shop exceeding the combined comfort benefit of all envelope measures (Zhai et al., 2015, 2020). Effect sizes vary by building typology: load sensitive buildings (Assembly, Cab Trim, Weld) respond to all three drivers, while load resistant buildings (Engine, Machine) respond primarily to roof insulation for energy and show minimal thermal comfort response to any passive measure.

LPD at the ASHRAE 90.1 / ECBC baseline (9.7 W/m²) increases EUI by ~20 kWh/m² relative to the as built specification, the largest single parameter energy penalty in the study. The as built design already exceeds the IGBC Green Factory LPD requirement by a substantial margin, confirming sound design stage decision making.

Shift scheduling has a mean effect of ~6 kWh/m²: two daytime shifts consistently outperform a day-night split because the night shift eliminates the daylighting contribution of the skylights, requiring full artificial lighting for the entire second shift. The Engine Shop is the sole exception, where cooling load reduction from cooler night time outdoor temperatures approximately offset the increased lighting load. This finding highlights that shift scheduling is an equal energy driver to roof insulation in naturally ventilated industrial buildings.

In the Assembly Shop, Cab Trim Shop, and the Weld Shop, the objectives are broadly aligned: the same parameter combinations (low LPD, Shift A, insulated roof) that minimise EUI also reduce discomfort hours, creating a Pareto front accessible through a single coherent design strategy. In the Engine Shop and Machine Shop, the two objectives are counterparts: energy can be reduced through passive measures, but comfort cannot be meaningfully improved by them. These buildings require active system upgrades or process level interventions.

Five recommendations follow from the evidence, in order of impact:

- Specify LPD below 7 W/m² at design stage. This is the highest return single decision for both energy and comfort, with an EUI premium of ~20 kWh/m² for non-compliance and a cascade benefit through reduced cooling loads and discomfort hours.
- Install roof insulation in all buildings but pair it with mechanical or passive night ventilation in buildings with process heat loads >40 W/m². Insulation without night ventilation creates a comfort penalty in the Weld Shop typology.

- Schedule both operational shifts during daytime hours wherever production planning permits. The ~6 kWh/m² energy benefit of two daytime shifts is achievable without capital investment and is recoverable through operational policy alone.
- Prioritise HVLS fan coverage in all naturally ventilated and evaporatively cooled buildings. Fan operation at AS1 airspeed reduces discomfort hours by more than any envelope measure. This is the facility's most impactful comfort asset.
- Classify buildings into load sensitive and load resistant typologies before investing in passive envelope upgrades. For load resistant buildings (high equipment to LPD ratio), passive measures will not achieve thermal comfort targets and active system upgrades should be scoped at design stage.

4.1 Broader Contribution

This study makes two contributions to the broader evidence base on Indian industrial buildings. First, it creates a functional IMAC-W framework; integrating IMAC, workshop field data and HVLS fan physics and validates its application across five building typologies within a single calibrated energy model (Kumar et al., 2020, 2021; Manu et al., 2016; Zhai et al., 2015, 2020).

Second, it provides evidence from a recently commissioned (2021) facility that the as built design of modern Indian industrial construction already approaches the efficiency boundary for passive measures, with the original case falling within 2% of best case EUI across all five buildings.

The facility studied represents 47,200 m² of the 22.1 million sq. ft of Grade A manufacturing floor space leased in India in 2024 (Sharma, 2025). With floor space projected to reach 34 million sq. ft by 2027, the design decisions documented here; LPD specification, roof insulation, shift scheduling, and HVLS fan coverage can be replicated across tens of millions of square metres of new construction in the composite climate zone in the near future. The five recommendations above are transferable to this broader population of facilities.

4.2 Limitations

The findings of this study are subject to several modelling and contextual constraints that should be considered when applying the results to other buildings or design contexts.

The energy model uses a simplified zone structure. Each building is divided into a small number of zones connected by air wall openings to simulate mixing, but this approach cannot fully capture the spatial variability in air temperature, humidity, and air movement that would occur across the large floor areas of these shops. Conditions near supply diffusers and in areas remote from cooling equipment will differ from the zone averaged values reported here.

The evaporative cooling system is represented using an ideal air loads model with constrained supply temperatures rather than a physically detailed evaporative cooler model. The actual cooling effectiveness of the installed evaporative units will vary with outdoor humidity conditions, and the simulated results may overestimate performance on high humidity days and underestimate it on dry days. A sensitivity analysis across different supply air temperatures would improve confidence in the comfort results.

The Ideal Air Loads system outputs net thermal cooling energy rather than electrical consumption. For buildings with evaporative coolers, this overestimates cooling electricity by a factor approximately equal to the system COP (~3). Since cooling contributes a minor share of total EUI relative to lighting and equipment loads, this does not affect the relative ordering of parametric scenarios but means absolute EUI values should be treated as approximate.

The study is limited to a single climate file representing Bhopal. The three parameter energy hierarchy and the comfort typology findings may not generalise directly to industrial buildings in other Indian climate zones, particularly humid coastal climates where evaporative cooling performance is substantially lower.

Infiltration rates are estimated values and have not been validated through pressurisation testing. Industrial buildings with frequent door openings and loading bays may have substantially higher infiltration than assumed, which would alter both the energy balance and the comfort results.

The parametric study does not include occupant behaviour or adaptive responses such as manual adjustment of fan speed, opening of louvres, or informal shading. These behaviours are common in Indian manufacturing environments and may significantly modify actual comfort outcomes relative to the simulated values.

4.3 Recommendations for Future Work

The most immediate research priority is the validation of the IMAC-W comfort framework through occupant surveys conducted in the study buildings during the summer operating season. The 18-metric evaluation matrix developed in this study generates falsifiable predictions: for example, IMAC-W_{90_AS1} predicts that 39.8% of occupied hours in the Assembly Shop will be reported as thermally unacceptable at 90% confidence under minimum fan operation. A structured comfort survey following the CARBSE IMAC protocol would allow this prediction to be tested and the IMAC-W threshold corrections to be refined or confirmed for the composite climate of Bhopal (Manu et al., 2016; Rawal et al., 2022).

The IMAC based comfort predictions should be validated through occupant surveys conducted during the summer operating season. A structured survey using the CBE Thermal Comfort Tool protocol or the CARBSE IMAC survey methodology would allow the modelled percentage of uncomfortable hours to be compared against reported thermal acceptability and would also capture the role of local air movement from HVLS fans, which is difficult to model in zone based simulations.

Replacing the ideal air loads representation with a physics based evaporative cooler model, including humidity dependent effectiveness and duct distribution losses, would improve the reliability of comfort predictions and allow the influence of outdoor humidity on seasonal comfort to be characterised.

The factory is designed for three shift operation but was modelled under two shift conditions reflecting current practice. Extending the parametric analysis to include a three shift continuous scenario would determine whether the energy and comfort outcomes remain in the same relative order and whether the night shift comfort penalty identified in this study intensifies or diminishes under continuous operation.

Applying the same parametric framework to equivalent industrial buildings in other Indian climate zones; Hot Dry (Ahmedabad), Hot Humid (Chennai), and Warm Humid (Mumbai) would establish whether the three parameter energy hierarchy and the two typology comfort classification identified here are robust features of the building type or are specific to the composite climate of Bhopal.

The PV simulation results generated in this study have not been fully integrated into the energy analysis. A net EUI assessment that combines demand side optimisation with roof mounted PV generation would provide a more complete picture of the facility's potential to meet Indian Green Building (IGBC) certification thresholds and would identify whether the most energy intensive buildings can achieve net zero or near zero annual energy balance through the combination of passive measures and on site generation.

This study evaluates design measures solely based on annual energy use and thermal comfort, without accounting for the capital cost of implementation, operational maintenance costs, or the embodied carbon of materials. A life cycle cost (LCC) analysis would reorder several of the findings: roof insulation, for example, carries a low material cost relative to its energy savings and would likely emerge as the highest return investment, while high performance triple glazed windows may show a poor payback period despite their modest EUI benefit. Conversely, a life cycle assessment (LCA) examining embodied carbon would add a further dimension; insulation materials with high global warming potential may offset their operational carbon savings over a 20 year - 30 year horizon in a low carbon grid scenario. Integrating LCC and LCA into the parametric framework would allow the 385 scenarios to be evaluated not just on energy and comfort performance but on whole life cost and carbon, providing a decision making tool that is directly actionable for facility developers and procurement teams operating under India's evolving green building and sustainability reporting requirements.

5 References

American Society of Heating, Refrigerating and Air-Conditioning Engineers. (2013). *Standard 55-2013: Thermal Environmental Conditions for Human Occupancy*. ASHRAE.

American Society of Heating, Refrigerating and Air-Conditioning Engineers. (2016). *Standard 90.1-2016: Energy Standard for Buildings Except Low-Rise Residential Buildings.* ASHRAE.

Bishoyi, D., & Sudhakar, K. (2017). Experimental performance of a direct evaporative cooler in composite climate of India. *Energy and Buildings*, *153*, 190–200. https://doi.org/10.1016/j.enbuild.2017.08.014

Bureau of Energy Efficiency (BEE). (2017). *Energy Conservation Building Code 2017*. Bureau of Energy Efficiency. https://beeindia.gov.in/WriteReadData/L45218/1734417634.pdf

Bureau of Indian Standards. (2016). *National Building Code of India: Volume 1*. Bureau of Indian Standards.

Chong, A., Gu, Y., & Jia, H. (2021). Calibrating building energy simulation models: A review of the basics to guide future work. *Energy and Buildings*, *253*, 111533. https://doi.org/10.1016/j.enbuild.2021.111533

Climate.OneBuilding. (2023). *IND_MP_Bhopal-Bhoj.AP.426670_TMYx.2009-2023* [Dataset]. https://climate.onebuilding.org/WMO_Region_2_Asia/IND_India/index.html

Dadras, Y., Mostafazadeh, F., Kavgic, M., & Ghobadi, M. (2025). Enhancing building energy optimization efficiency: A performance analysis of simplification approaches. *Journal of Building Engineering*, *105*, 112559. https://doi.org/10.1016/j.jobe.2025.112559

Das, D., & Lolla, A. (2024). *Green electrification of Indian industries for clean energy gains*. Ember Energy. https://ember-energy.org/app/uploads/2024/09/Report-Green-electrification-of-Indian-industries-for-clean-energy-gains.pdf

de Dear, R. J. (1998). *Developing an Adaptive Model of Thermal Comfort and Preference*.

Ecoair. (2024a). *HVLS Fans*. Ecoair Cooling Systems Pvt. Ltd. https://www.ecoair.co.in/products/geared-hvls-fans/

Ecoair. (2024b). *Wall Mounted HVLS Fans*. Ecoair Cooling Systems Pvt. Ltd. https://www.ecoair.co.in/products/wall-mounted-hvls-fan/

Energy Transitions Commission. (2020). *Making Mission Possible: Delivering a Net-Zero Economy*. Energy Transitions Commission (ETC). https://www.energy-transitions.org/wp-content/uploads/2020/09/Making-Mission-Possible-Full-Report.pdf

Gagge, A., Fobelets, A., & Berglund, L. (1986). A standard predictive index of human response to the thermal environment. *Ashrae Transactions*. https://www.semanticscholar.org/paper/A-standard-predictive-index-of-human-response-to-Gagge-Fobelets/af4d93cb49790780a30c758d7af92dc8daa72b9e

Gagge, A., Stolwijk, J., & Nishi, Y. (1972, May 1). *An Effective Temperature Scale Based on a Simple Model of Human Physiological Regulatiry Response*. https://www.semanticscholar.org/paper/An-Effective-Temperature-Scale-Based-on-a-Simple-of-Gagge-Stolwijk/5ca3afa7ed2167f1c1d6105fd91e3f069bd32f64

Gandhi Automation Pvt. Ltd. (2025). *Rolling Shutters*. Gandhi Automation Pvt. Ltd.

Gentle, A. R., Aguilar, J. L. C., & Smith, G. B. (2011). Optimized cool roofs: Integrating albedo and thermal emittance with *R*-value. *Solar Energy Materials and Solar Cells*, *95*(12), 3207–3215. https://doi.org/10.1016/j.solmat.2011.07.018

Government of India. (2019). *India Cooling Action Plan (ICAP)*. Ministry of Environment, Forest and Climate Change (MoEFCC). https://ozonecell.nic.in/wp-content/uploads/2019/03/INDIA-COOLING-ACTION-PLAN-e-circulation-version080319.pdf

Government of India. (2020). *Finance Minister announces Government Reforms and Enablers across Seven Sectors under Aatma Nirbhar Bharat Abhiyaan*. PIB Delhi. https://www.pib.gov.in/www.pib.gov.in/Pressreleaseshare.aspx?PRID=1624661

International Energy Agency. (2018, October 18). *Market Report Series: Energy Efficiency 2018*. IEA. https://www.iea.org/reports/energy-efficiency-2018

International Energy Agency. (2021a). *India Energy Outlook 2021*. International Energy Agency. https://doi.org/10.1787/ec2fd78d-en

International Energy Agency. (2021b). *Net Zero by 2050—A Roadmap for the Global Energy Sector*.

International Energy Agency. (2023). *Buildings—Energy System*. International Energy Agency (IEA). IEA. https://www.iea.org/energy-system/buildings

International Organization for Standardization (ISO). (2004). *Ergonomics of the thermal environment—Determination of metabolic rate* (ISO 8996:2004; 2nd edition). ISO.

International Organization for Standardization (ISO). (2005). *Ergonomics of the thermal environment—Analytical determination and interpretation of thermal comfort using calculation of the PMV and PPD indices and local thermal comfort criteria* (ISO 7730:2005; 3rd edition). English.

Kumar, S., Mathur, A., Singh, M. K., & Rana, K. B. (2021). Adaptive thermal comfort study of workers in a mini-industrial unit during summer and winter season in a tropical country, India. *Building and Environment*, *197*, 107874. https://doi.org/10.1016/j.buildenv.2021.107874

Kumar, S., Mathur, J., Mathur, S., Singh, M. K., & Loftness, V. (2016). An adaptive approach to define thermal comfort zones on psychrometric chart for naturally ventilated buildings in composite climate of India. *Building and Environment*, *109*, 135–153. https://doi.org/10.1016/j.buildenv.2016.09.023

Kumar, S., Singh, M. K., Mathur, A., & Košir, M. (2020). Occupant's thermal comfort expectations in naturally ventilated engineering workshop building: A case study at high metabolic rates. *Energy and Buildings*, *217*, 109970. https://doi.org/10.1016/j.enbuild.2020.109970

Luo, M., Wang, Z., Ke, K., Cao, B., Zhai, Y., & Zhou, X. (2018). Human metabolic rate and thermal comfort in buildings: The problem and challenge. *Building and Environment*, *131*, 44–52. https://doi.org/10.1016/j.buildenv.2018.01.005

Manu, S., Shukla, Y., Rawal, R., Thomas, L. E., & De Dear, R. (2016). Field studies of thermal comfort across multiple climate zones for the subcontinent: India Model for Adaptive Comfort (IMAC). *Building and Environment*, *98*, 55–70. https://doi.org/10.1016/j.buildenv.2015.12.019

Michael, S., Rakheja, K., Garg, V., & Konda, C. (2025). *Meeting India's Peak Power Demand with Clean Energy*. The Institute for Energy Economics and Financial Analysis (IEEFA). https://ieefa.org/sites/default/files/2025-07/Meeting%20India%E2%80%99s%20Peak%20Power%20Demand%20with%20Clean%20Energy_0.pdf

NITI Aayog & Rocky Mountain Institute (RMI). (2020). *Towards A Clean Energy Economy: Post-COVID-19 Opportunities for India's Energy and Mobility Sectors*. https://www.niti.gov.in/sites/default/files/2023-02/India_Green_Stimulus_Report_NITI_VF_June_29.pdf

Rawal, R., Shukla, Y., Vardhan, V., Asrani, S., Schweiker, M., de Dear, R., Garg, V., Mathur, J., Prakash, S., Diddi, S., Ranjan, S. V., Siddiqui, A. N., & Somani, G. (2022). Adaptive thermal comfort model based on field studies in five climate zones across India. *Building and Environment*, *219*, 109187. https://doi.org/10.1016/j.buildenv.2022.109187

Rawat, M., & Singh, R. N. (2022). A study on the comparative review of cool roof thermal performance in various regions. *Energy and Built Environment*, *3*(3), 327–347. https://doi.org/10.1016/j.enbenv.2021.03.001

Sabic. (2013). *LEXAN™ THERMOCLEAR™ Sheet Technical Manual*. Sabic.

Saint-Gobain Glass. (2025). *The Essential Glass for Facade*. Saint-Gobain Glass.

Sharma, M. (2025, December 3). India's manufacturing leasing to hit 46% of India's industrial real estate by 2027: JLL. *Fortune India*. https://www.fortuneindia.com/business-news/indias-manufacturing-leasing-to-hit-46-of-indias-industrial-real-estate-by-2027-jll/128514

Smallcombe, J. W., Ranhotty, R. N., Bach, A. J. E., Palutikof, J. P., Tonmoy, F. N., Joarder, A. R., Hossain, M., Morris, N. B., Capon, A., Mavros, Y., & Jay, O. (2025). Sustainable cooling strategies for workers in the ready-made garment factory industry in Bangladesh under simulated extreme heat: A randomised crossover trial. *The Lancet Planetary Health*, *9*(9), 101317. https://doi.org/10.1016/j.lanplh.2025.101317

The Indian Green Building Council (IGBC). (2025). *IGBC Green Factory Building Rating System Version 2.0*. The Indian Green Building Council (IGBC).

United Nations Environment Programme. (2024). *Global Status Report for Buildings and Construction - Beyond foundations: Mainstreaming sustainable solutions to cut emissions from the buildings sector*. United Nations Environment Programme. https://doi.org/10.59117/20.500.11822/45095

U.S. Department of Energy (DOE). (2025). *EnergyPlus™*. https://energyplus.net/

Verma, R., Kumar, S., Rakshit, D., & Udayraj. (2026). Integrated Evaluation of Passive Building Strategies through Experimental Analysis, Energy Simulation, and Life Cycle Assessment in the Composite Climate of India. *Case Studies in Thermal Engineering*, 107956. https://doi.org/10.1016/j.csite.2026.107956

Wang, H., Sun, L., Guan, H., & Hu, S. (2018). Thermal environment investigation and analysis on thermal adaptation of workers in a rubber factory. *Energy and Buildings*, *158*, 1625–1631. https://doi.org/10.1016/j.enbuild.2017.11.046

Zhai, Y., Elsworth, C., Arens, E., Zhang, H., Zhang, Y., & Zhao, L. (2015). Using air movement for comfort during moderate exercise. *Building and Environment*, *94*, 344–352. https://doi.org/10.1016/j.buildenv.2015.08.026

Zhai, Y., Zhao, S., Gao, Y., Song, W., Yang, L., Zhang, H., & Arens, E. (2020). Preferred temperatures with and without air movement during moderate exercise. *Energy and Buildings*, *207*, 109565. https://doi.org/10.1016/j.enbuild.2019.109565

Zingre, K. T., Wan, M. P., Tong, S., Li, H., Chang, V. W.-C., Wong, S. K., Thian Toh, W. B., & Leng Lee, I. Y. (2015). Modeling of cool roof heat transfer in tropical climate. *Renewable Energy*, *75*, 210–223. https://doi.org/10.1016/j.renene.2014.09.045

APPENDIX A - ARCHITECTURAL DRAWINGS

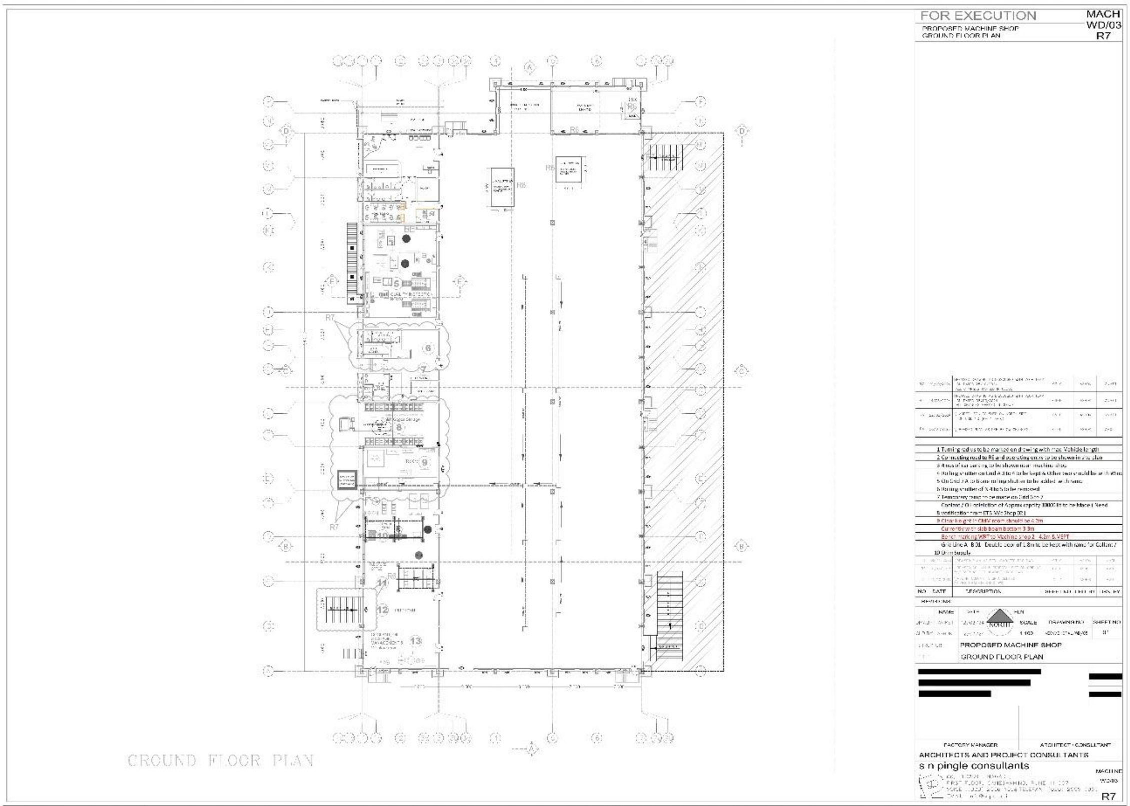

Figure 15. Machine Shop: Floor Plan

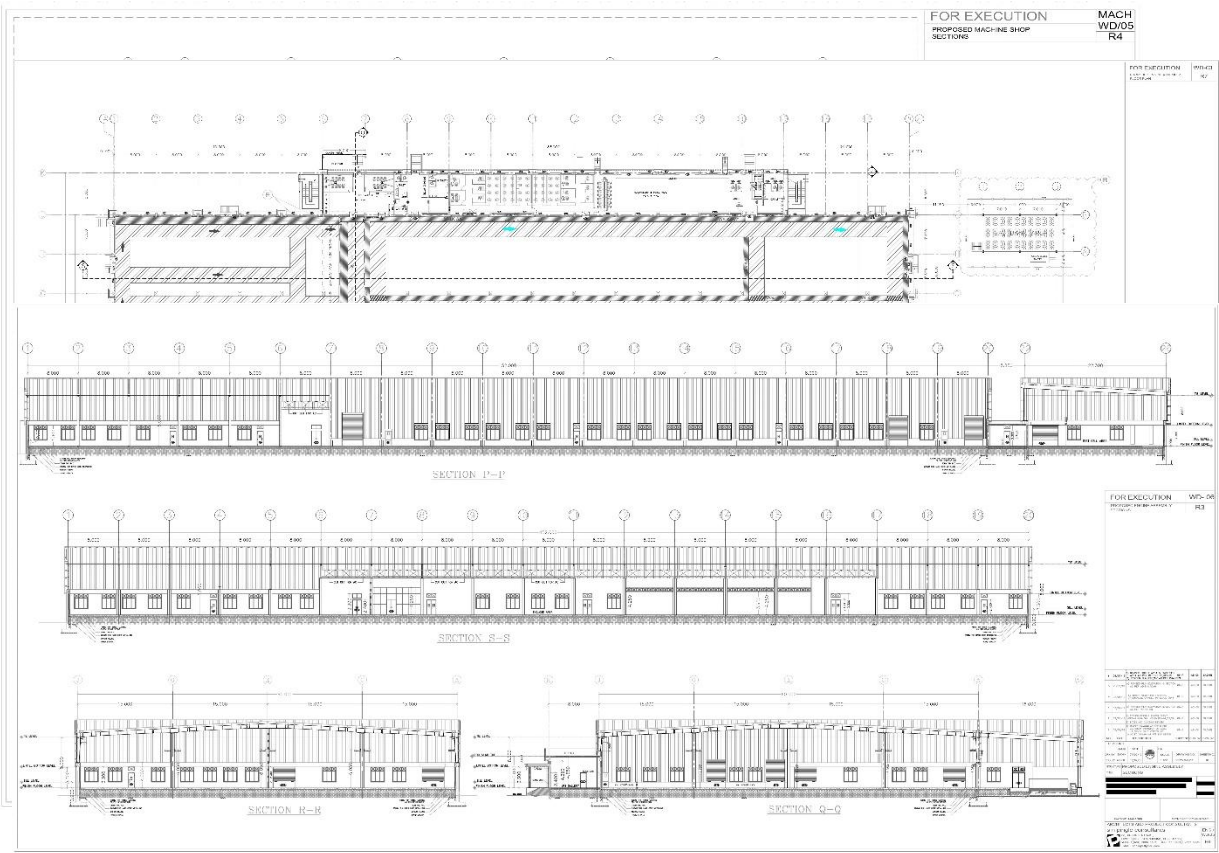

Figure 17. Engine Shop: Sections

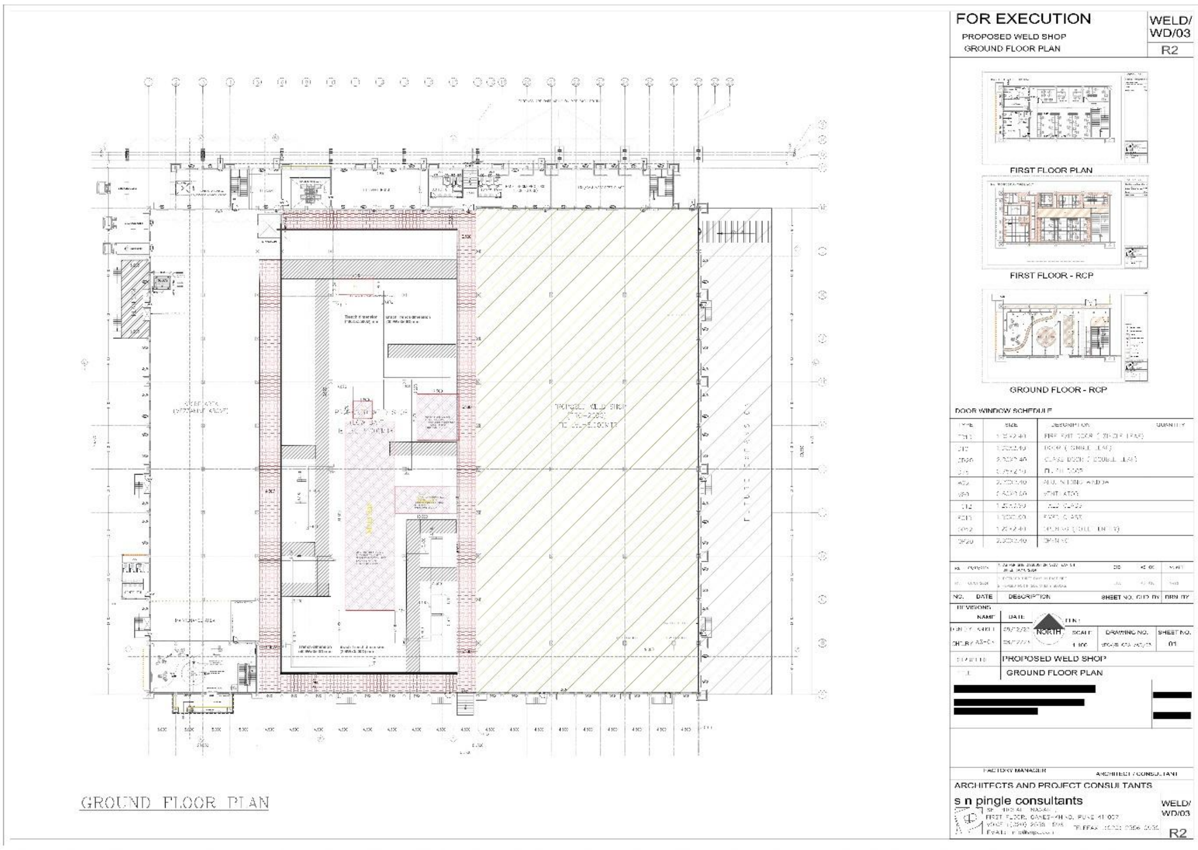

Figure 20. Weld Shop: Floor Plan

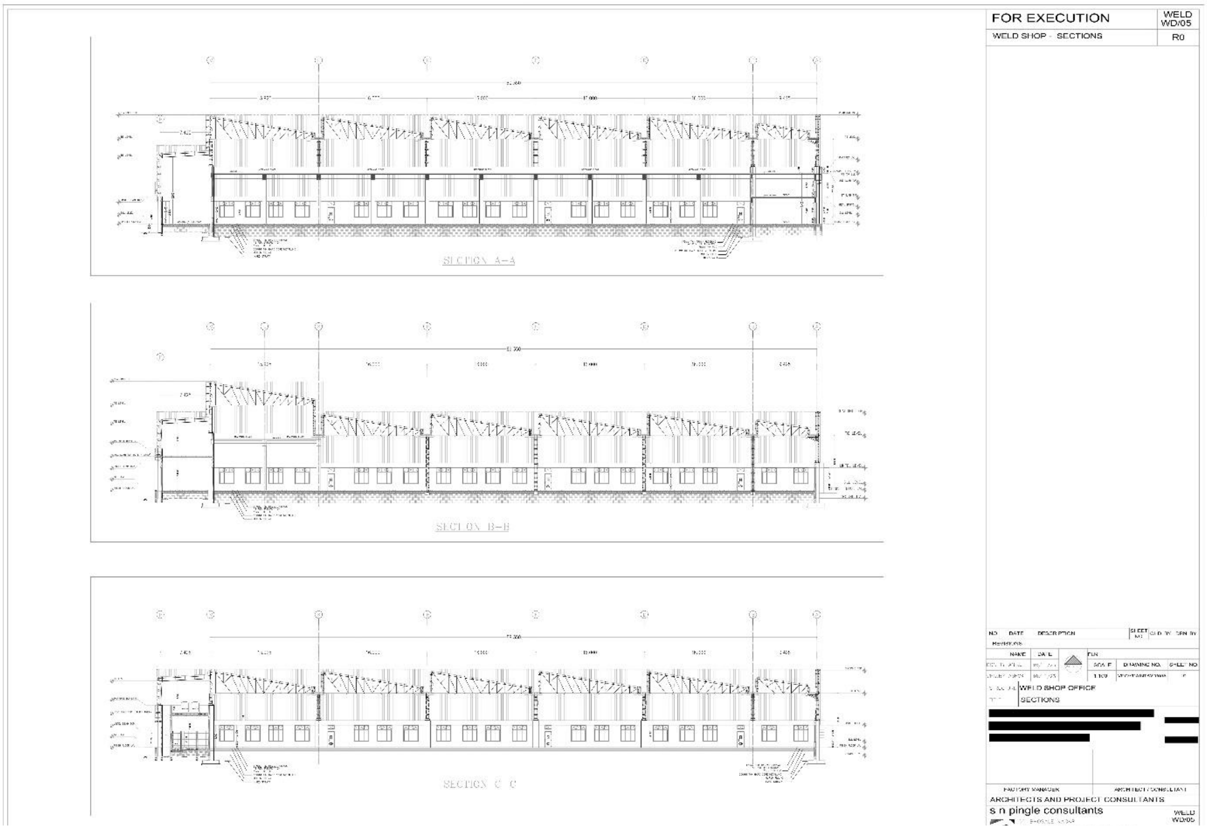

Figure 19. Weld Shop: Sections

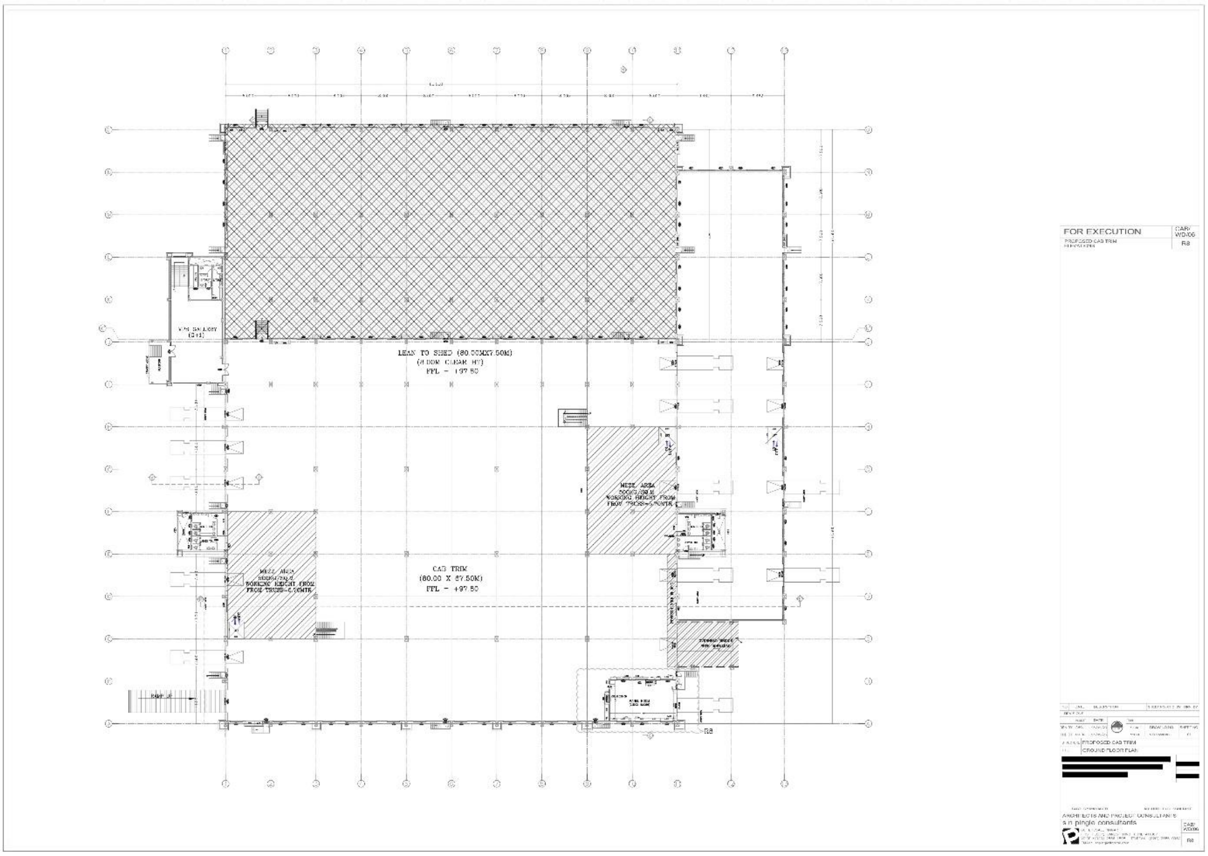

Figure 21. Cab Trim: Floor Plan

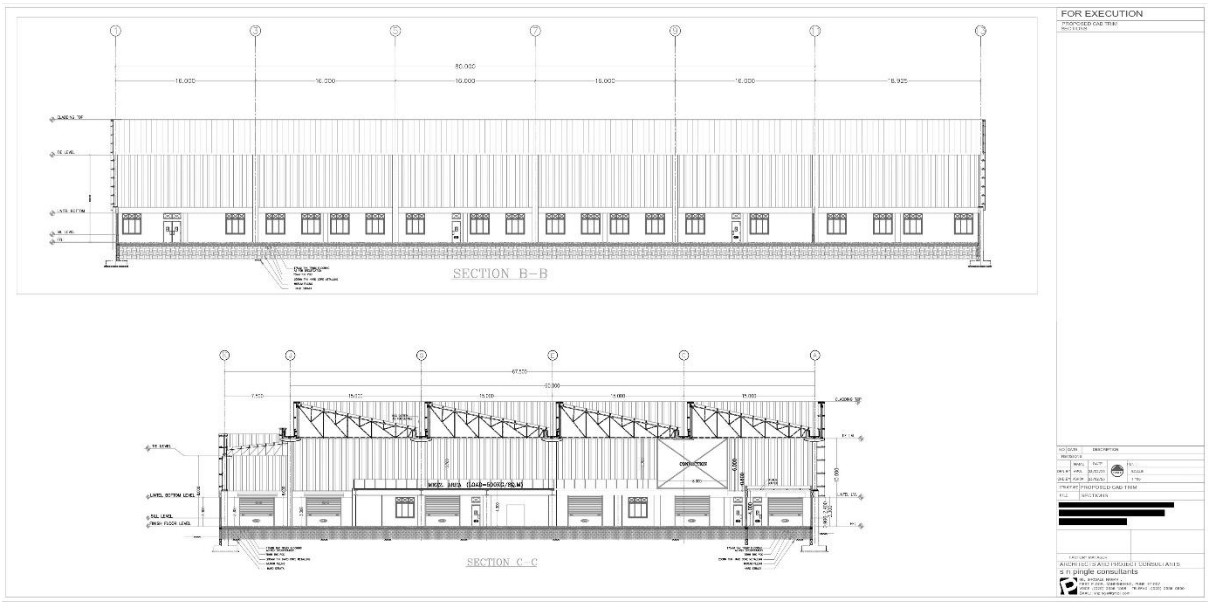

Figure 22, Cab Trim: Sections

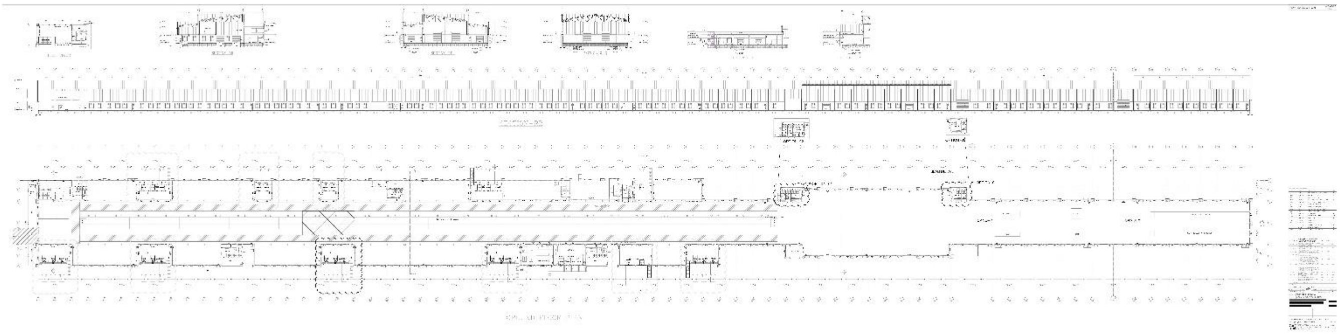

Figure 23. Assembly Shop: Floor Plan and Sections

APPENDIX B – GRAPHS AND DATA

EUI EFFECT

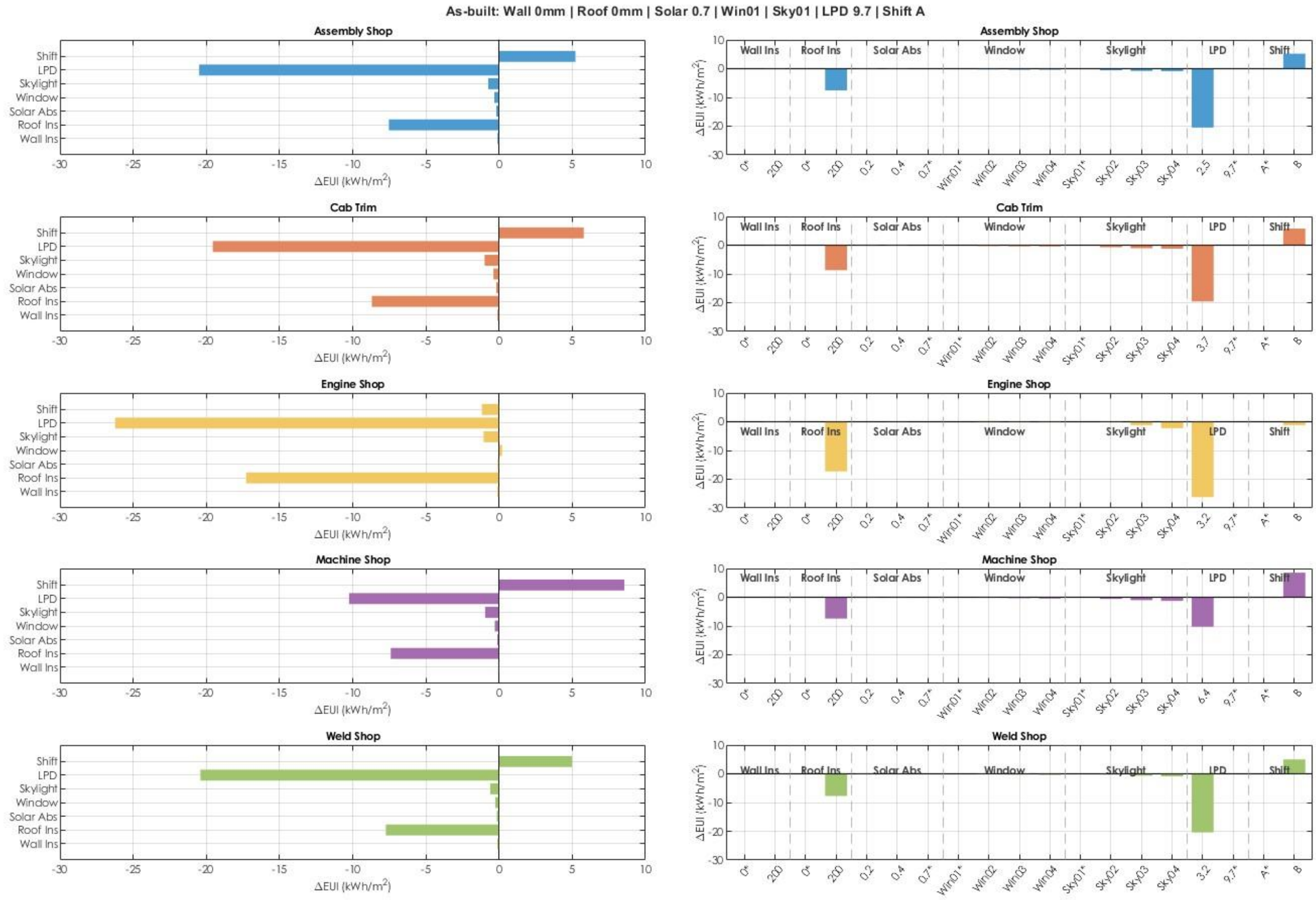

Figure 24. Mean ΔEUI per measure (left) and per level of each measure (right)

THERMAL COMFORT METRIC VISUALISATION

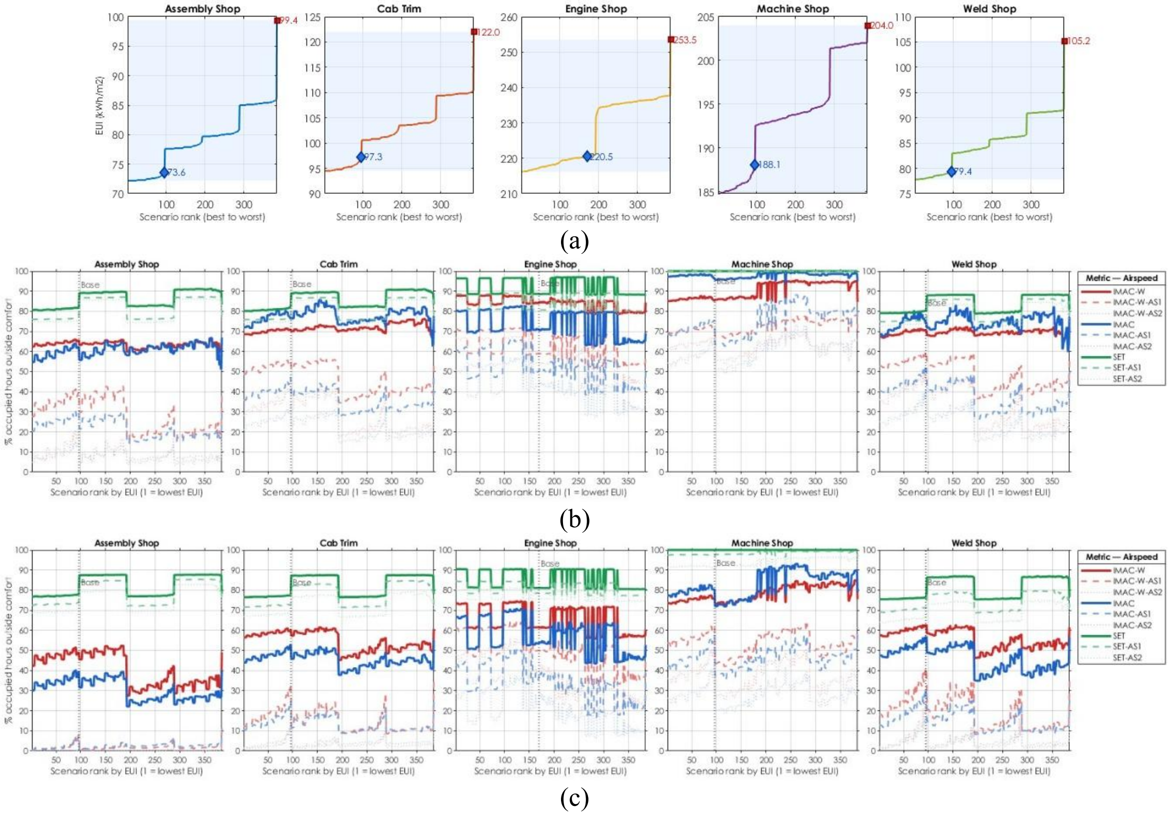

Figure 25. (a) EUI in increasing order per building; thermal comfort percentage of each metric as per increasing EUI in (b) 90% comfort band and (c) 80% comfort band

THERMAL COMFORT METRIC COMPARISON

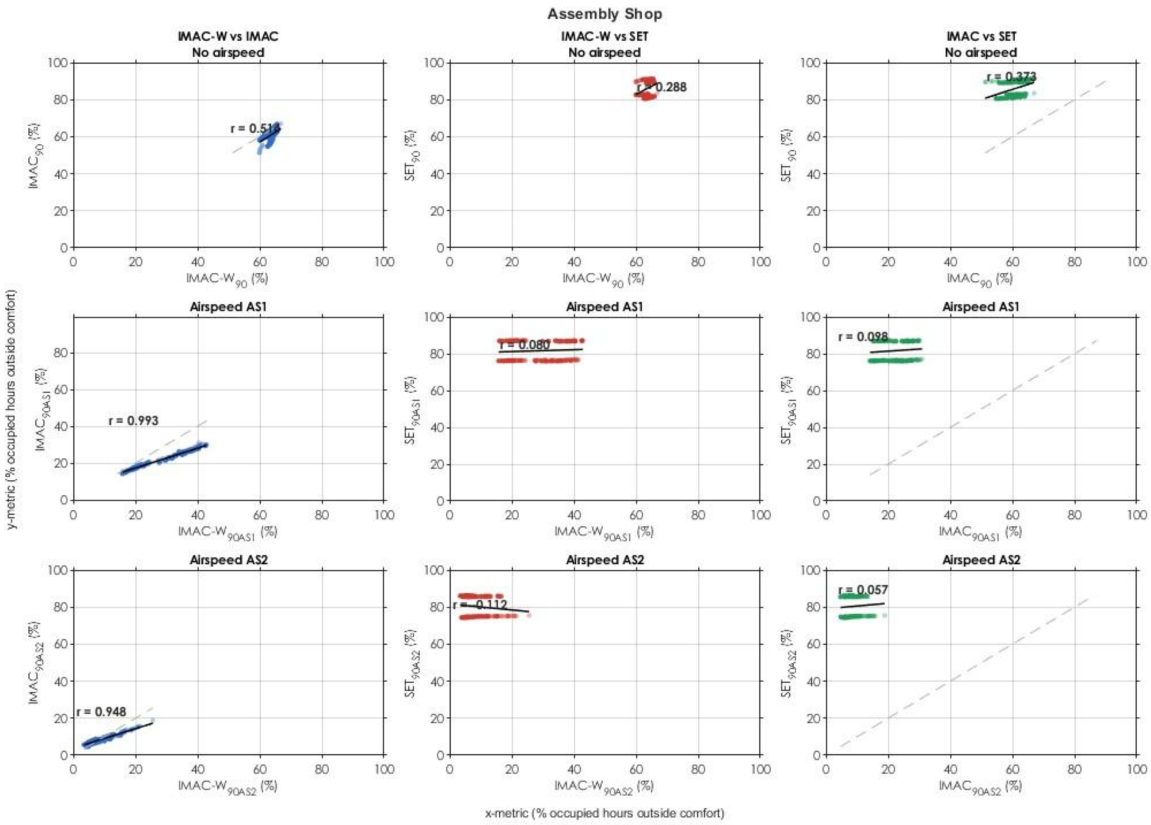

Figure 26. 90% thermal comfort metric correlation - Assembly Shop

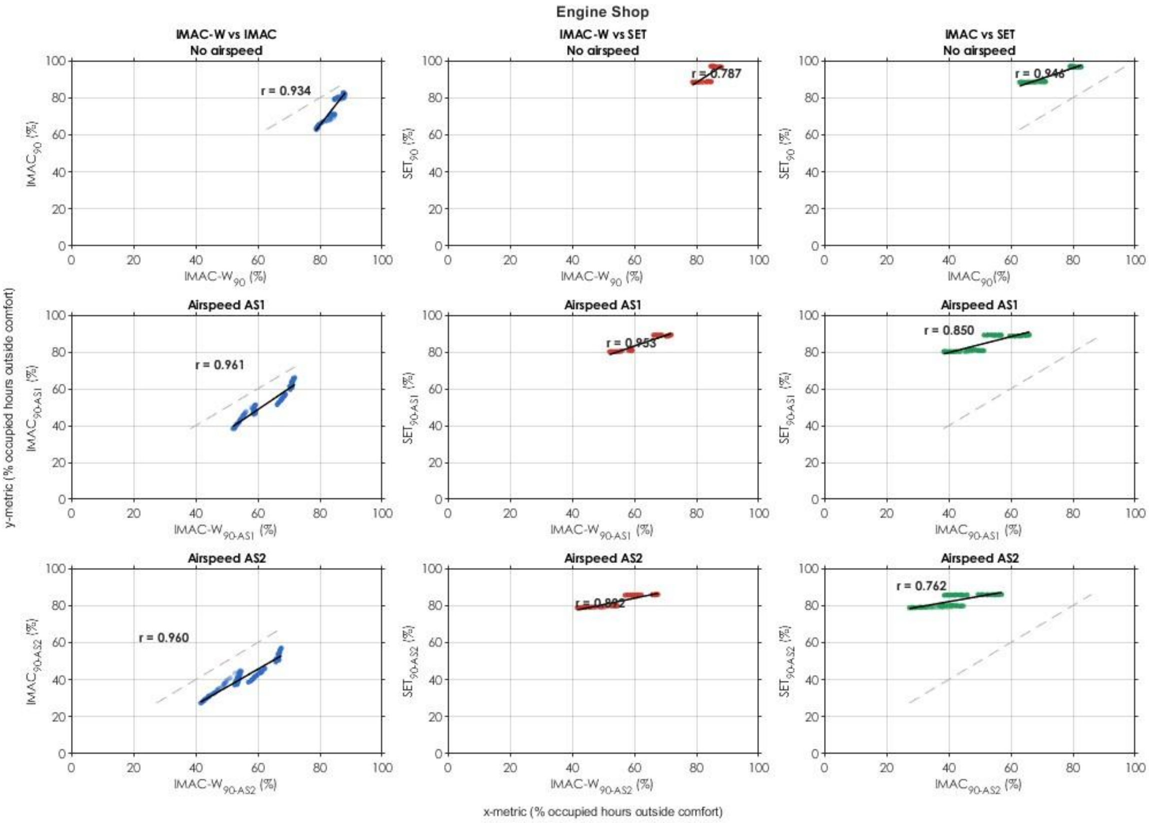

Figure 27. 90% thermal comfort metric correlation - Engine Shop

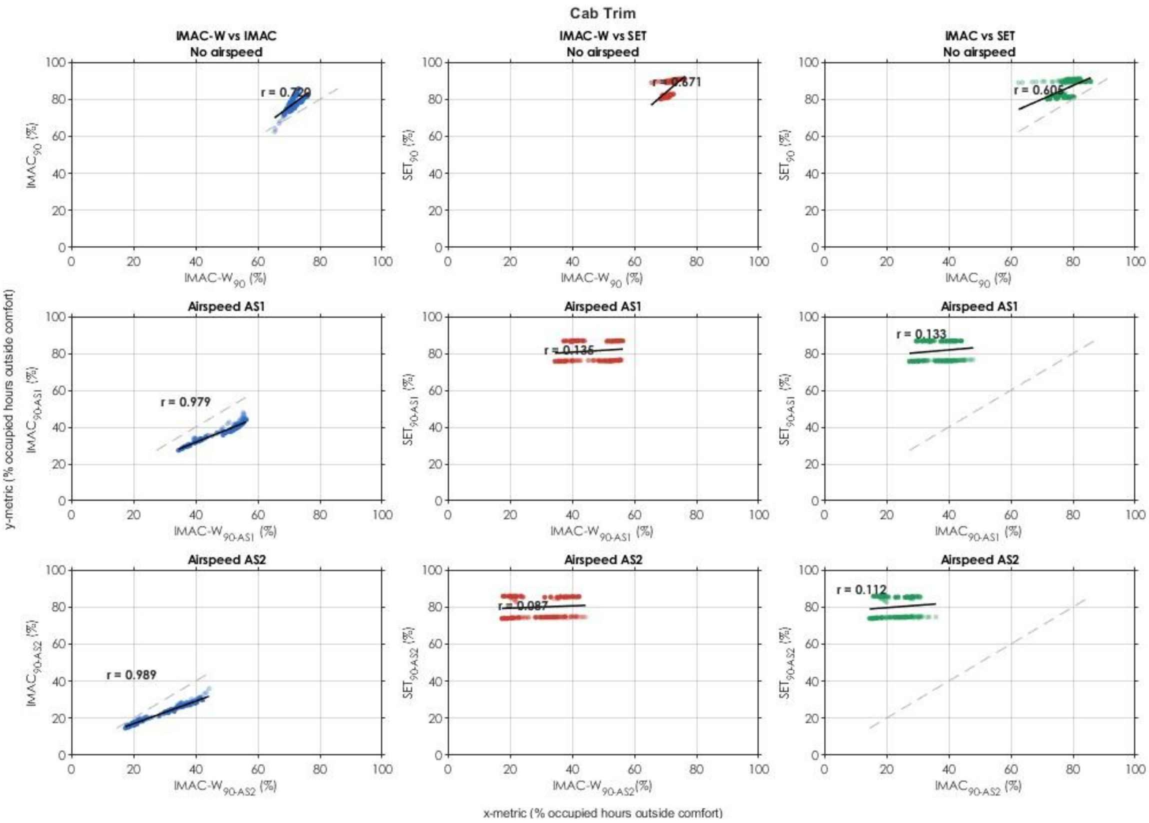

Figure 28. 90% thermal comfort metric correlation - Cab Trim

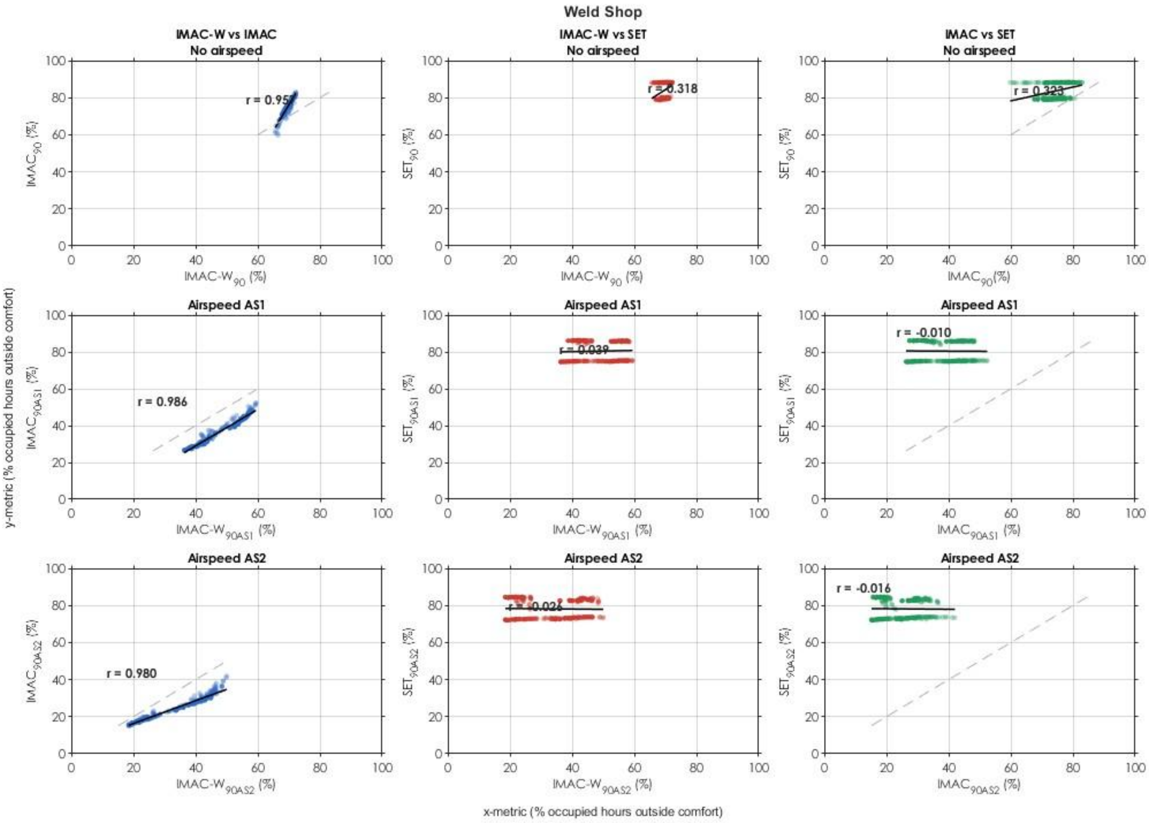

Figure 29. 90% thermal comfort metric correlation - Weld Shop

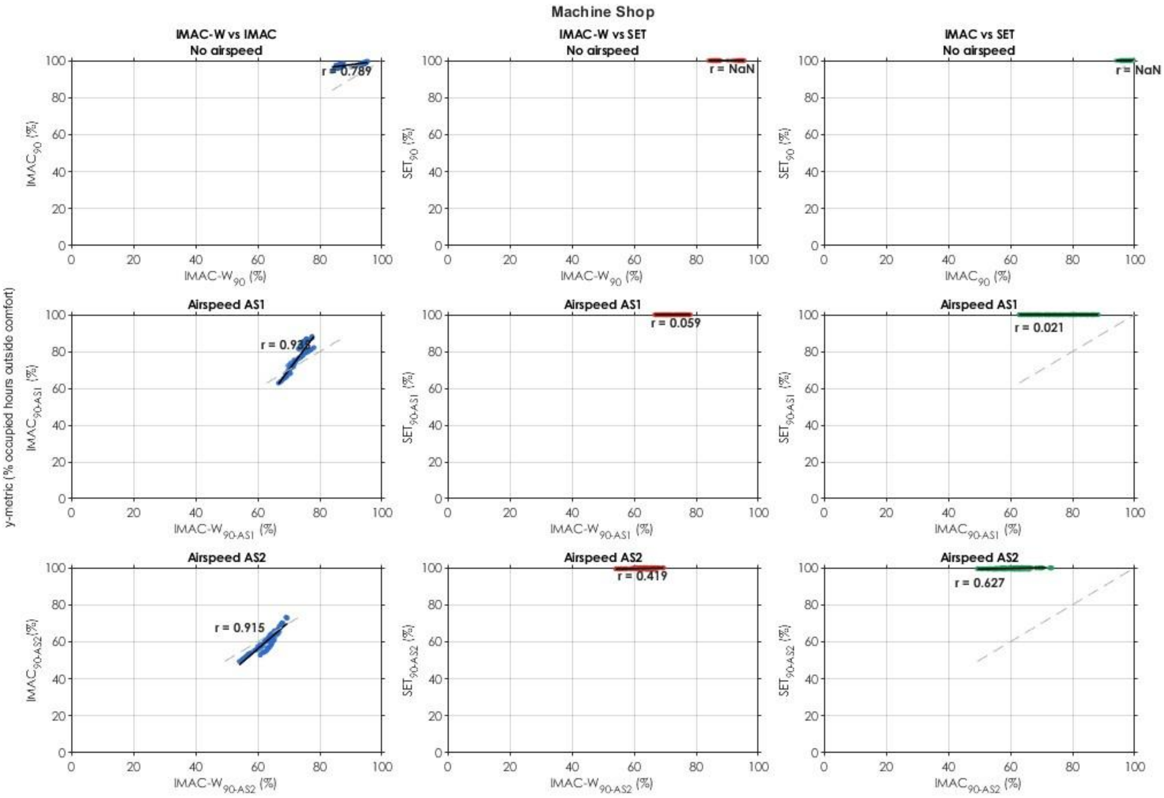

Figure 30. 90% thermal comfort metric correlation - Machine Shop

THERMAL COMFORT RESPONSE BY MEASURE COMPARISON FOR ALL METRICS

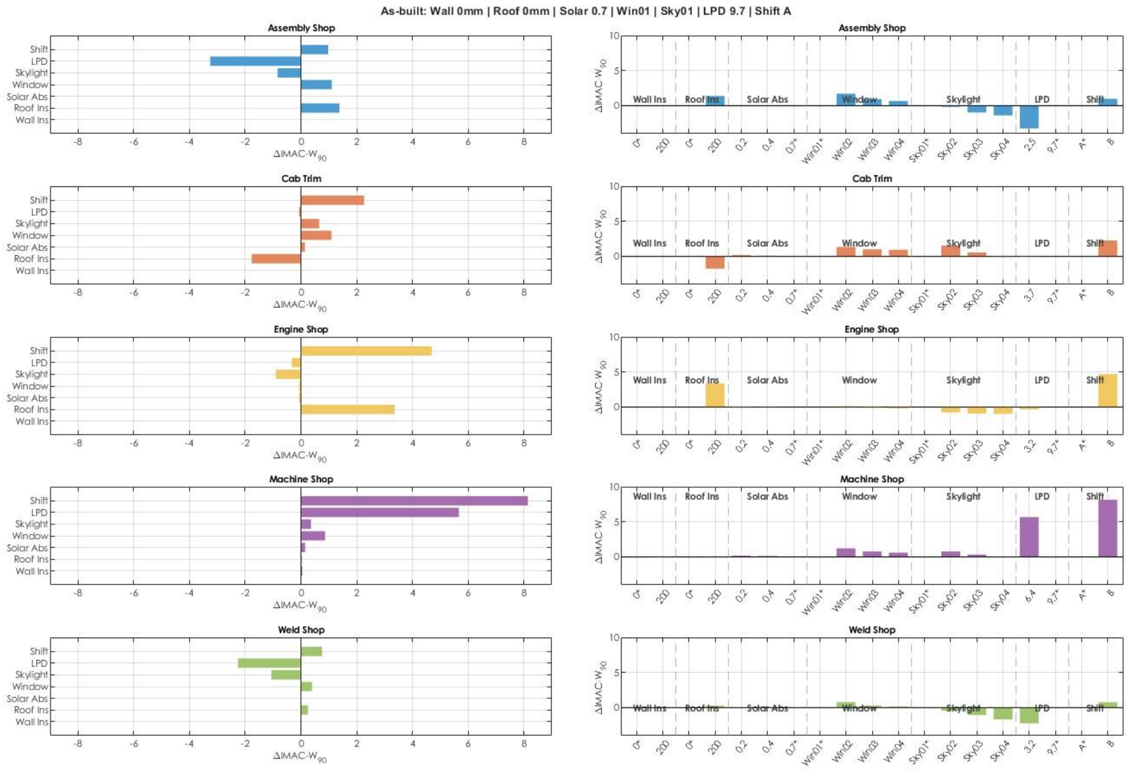

Figure 31. Mean ΔIMAC-W_{90} per measure (left) and per level of each measure (right)

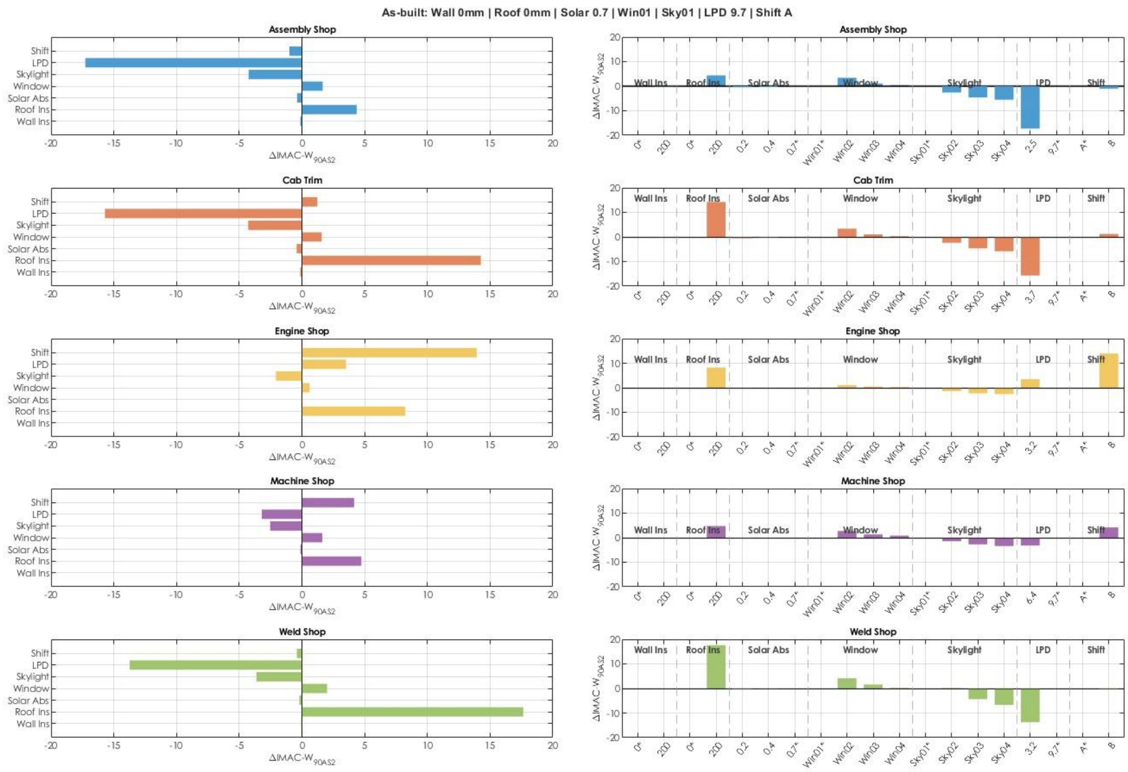

Figure 32. Mean ΔIMAC-W_{90AS2} per measure (left) and per level of each measure (right)

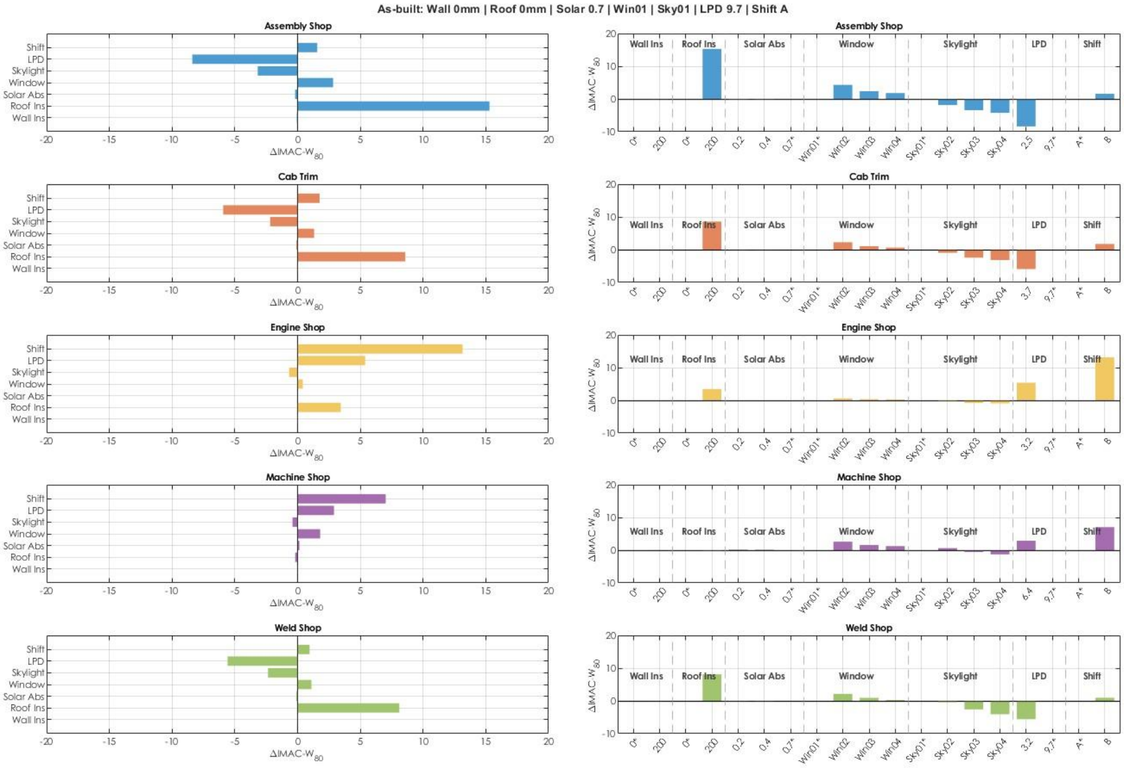

Figure 33. Mean ΔIMAC-W_{80} per measure (left) and per level of each measure (right)

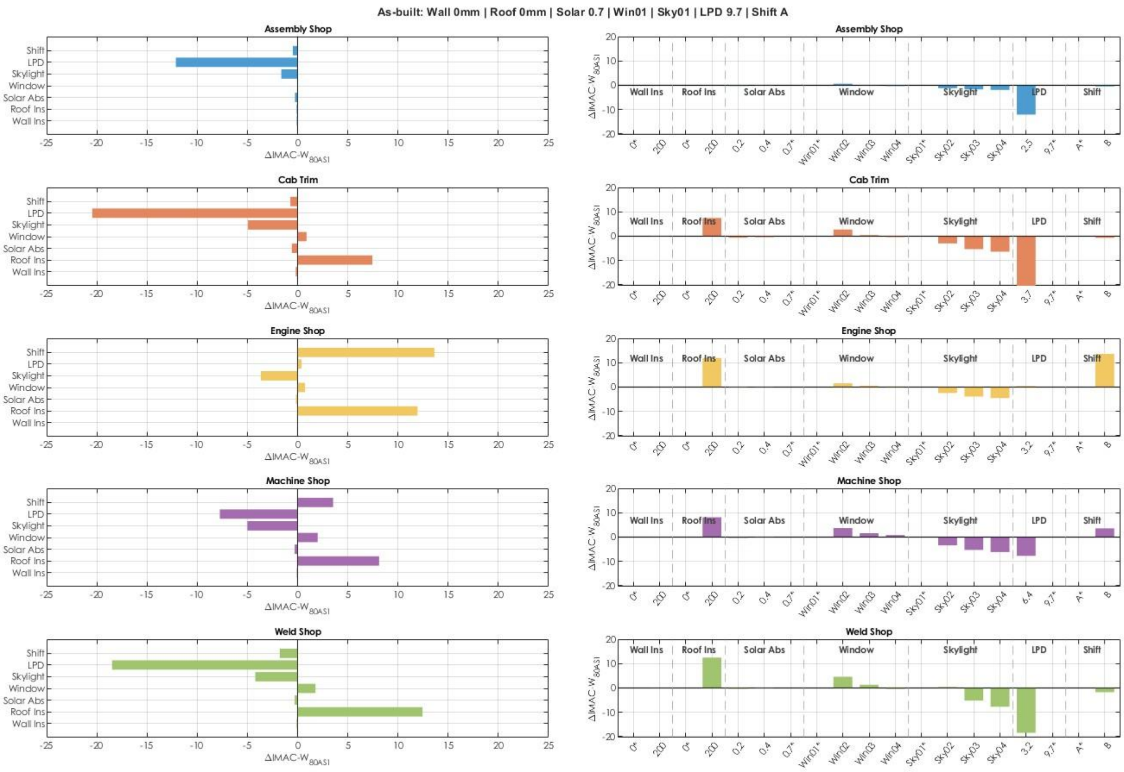

Figure 34. Mean ΔIMAC-W_{80AS1} per measure (left) and per level of each measure (right)

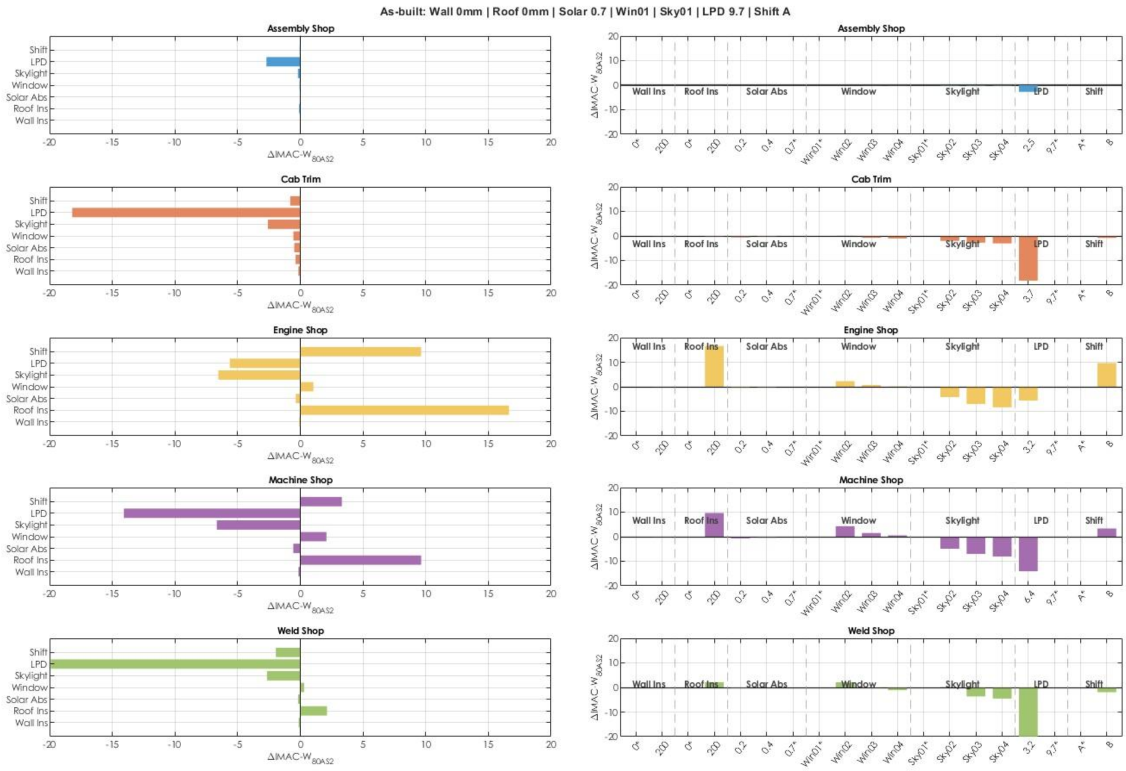

Figure 35. Mean ΔIMAC-W80AS2 per measure (left) and per level of each measure (right)

PARETO PLOTS FOR ALL COMFORT BANDS

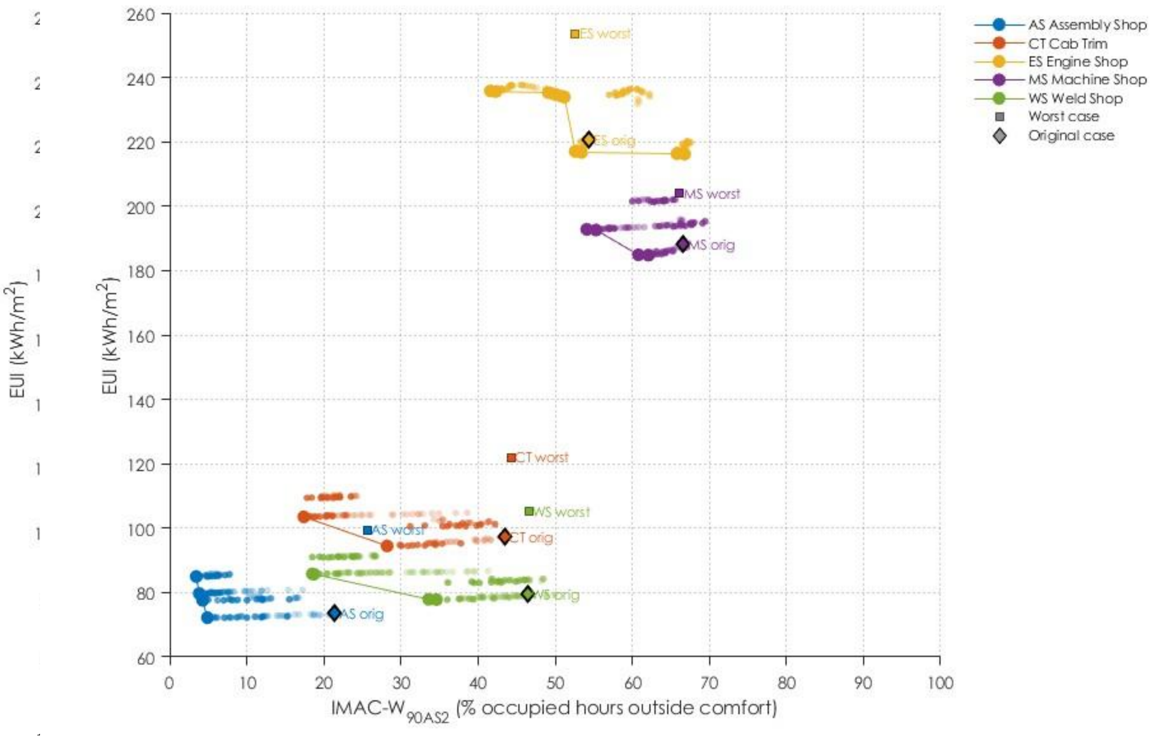

Figure 36. EUI x Thermal Comfort plot (IMAC-W$_{90AS2}$) with pareto fronts for all buildings

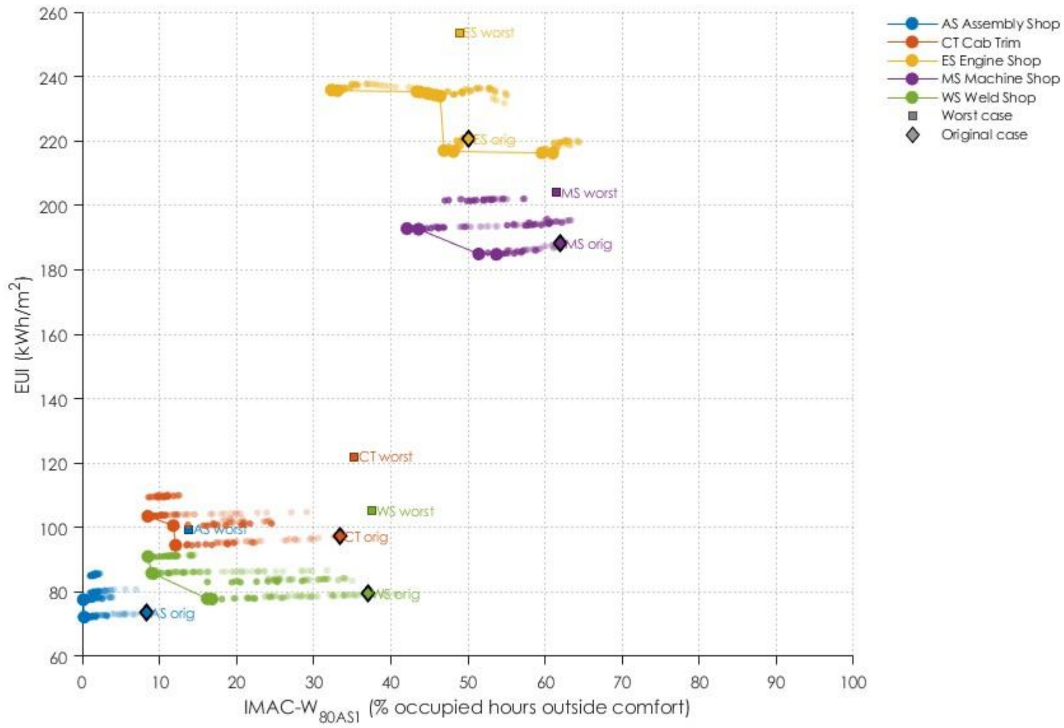

Figure 38. EUI x Thermal Comfort plot (IMAC-W$_{80AS1}$) with pareto fronts for all buildings

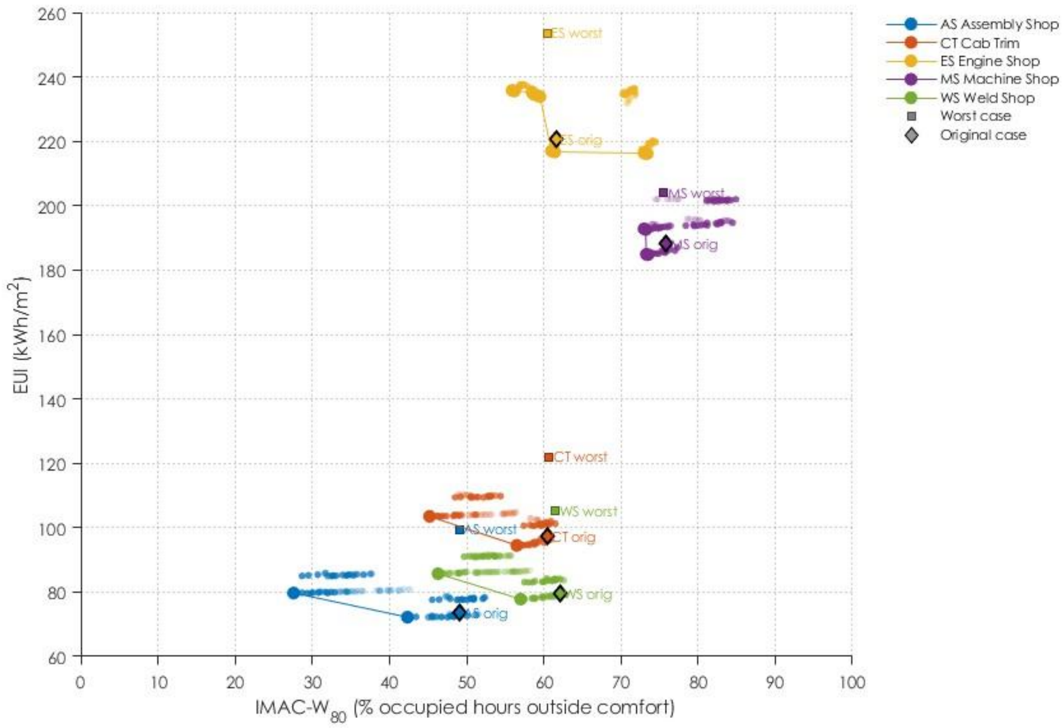

Figure 39. EUI x Thermal Comfort plot (IMAC-W$_{80}$) with pareto fronts for all buildings

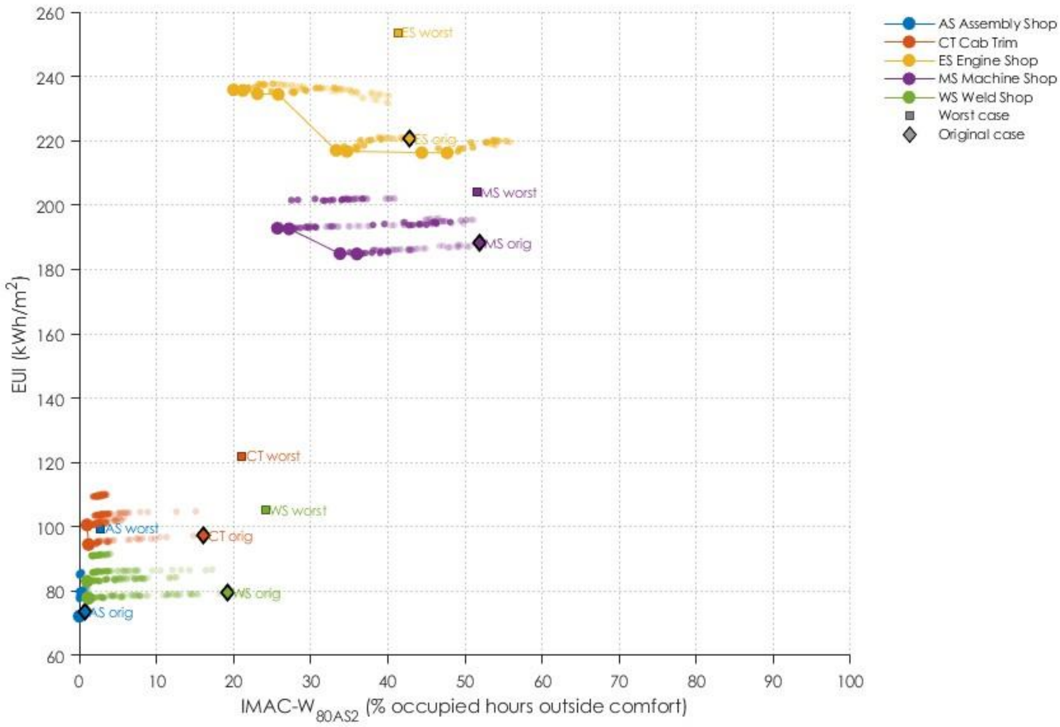

Figure 40. EUI x Thermal Comfort plot (IMAC-W_{80AS2}) with pareto fronts for all buildings

APPENDIX C - SITE PHOTOGRAPHS

Figure 41. Aerial View (West): Industry campus

Figure 42. Aerial View (Top): Assembly Shop

Figure 43. Aerial View (North): Machine Shop

Figure 44. Aerial View (North): Weld Shop

Figure 45. Aerial View (North-East): Machine, Engine Shop, Weld Shop (left to right)

Figure 46. Machine Shop: Interior showing the northbay and roof skylights, and the interior lighting.

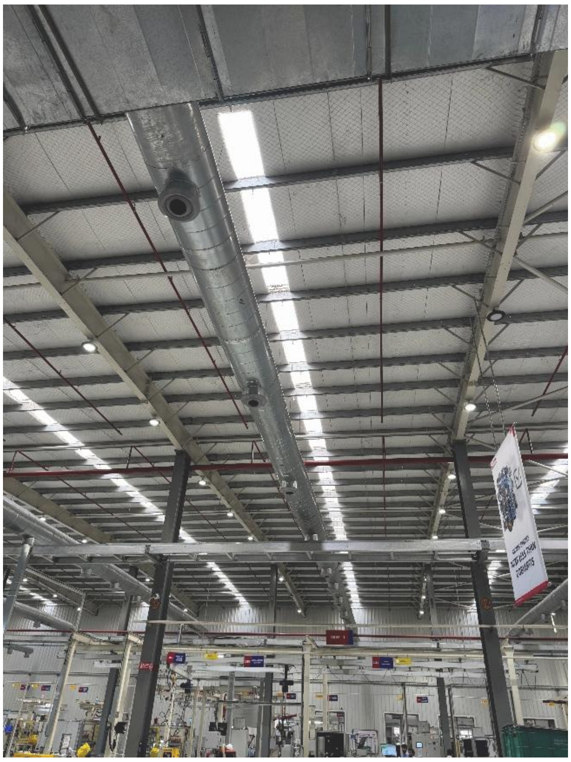

(a) **(b)**

Figure 48. Engine Shop: (a) Shop floor interior showing ducts and skylights; (b) HVAC ducts and roof skylights.

Figure 47. Weld Shop: Interior showing northbay and roof skylights.

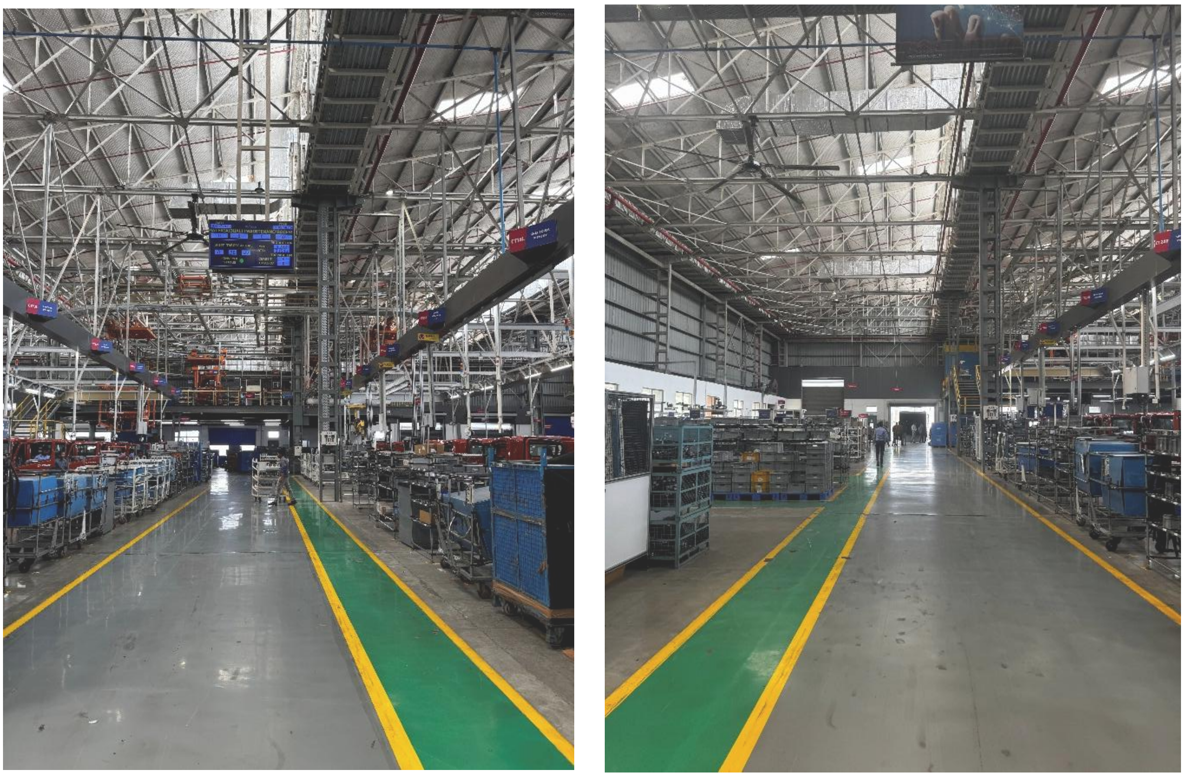

(a) (b)

Figure 49. Cab Trim: Interior showing the northbay and roof skylights, lighting fixtures, localised evaporative cooler ducts and HVLS fans.

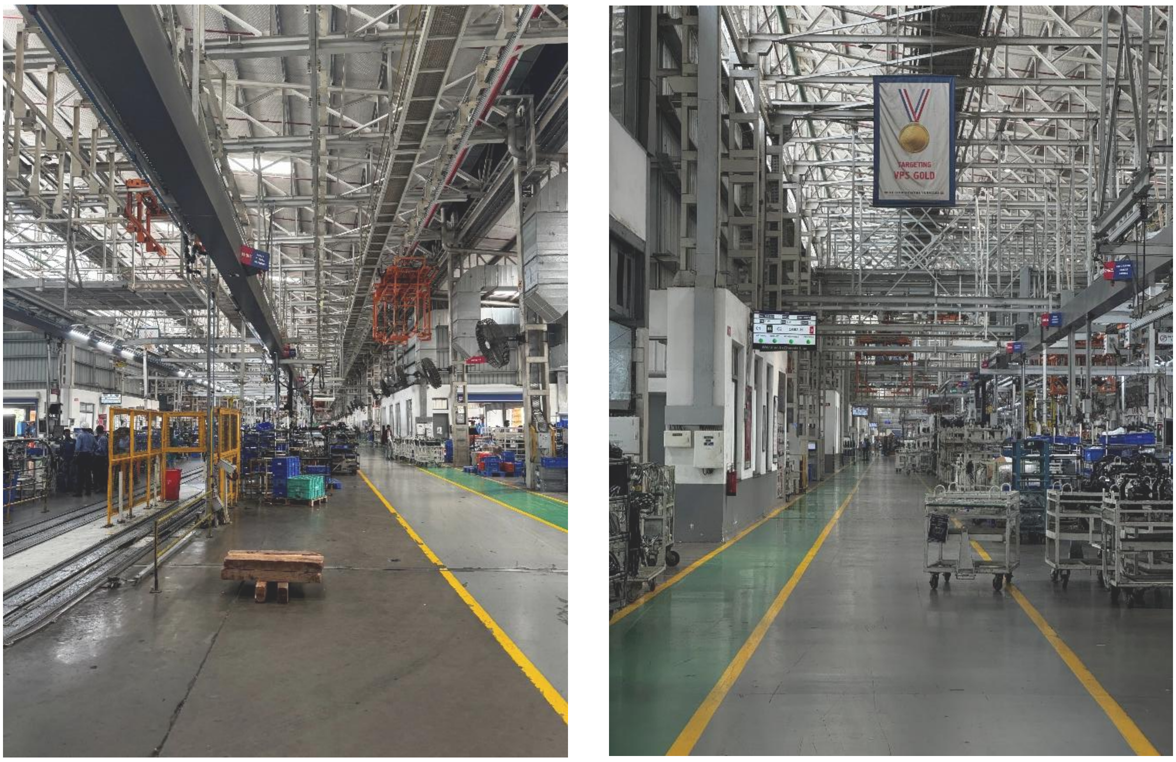

(a) (b)

Figure 50. Assembly Shop: Block A and B showing northbay and roof skylights, evaporative cooler ducts from AHU and HVLS fans.

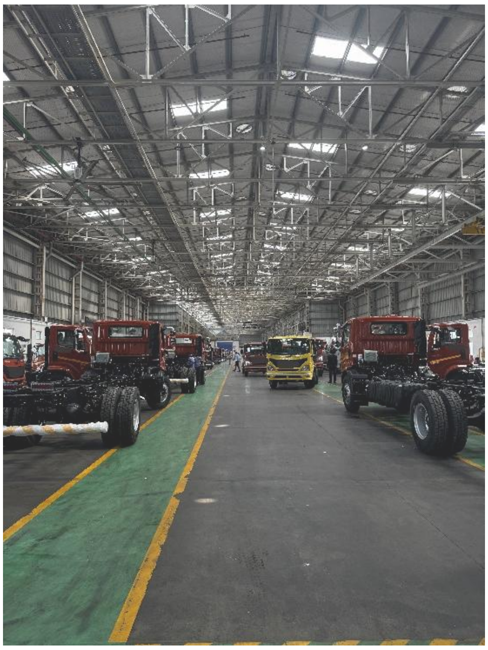

(a)

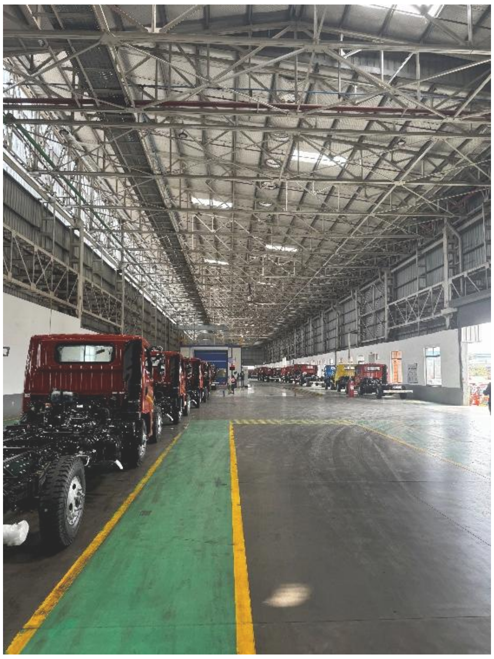

(b)

Figure 51.Assembly Shop: (a) Block C and (b) Block D; showing the roof type.

(a)

(b)

(c)

Figure 52. Evaporative Cooler AHU; (a) interior fresh air section; (b) and (c) external view showing the different sections of the AHU.

(a)

(b)

(c)

Figure 53. (a) Evaporative Cooler AHU;s on the exterior of the Assembly Shop; localised evaporative coolers installed on the (b) roof and (c) on the service roof slab

(a)

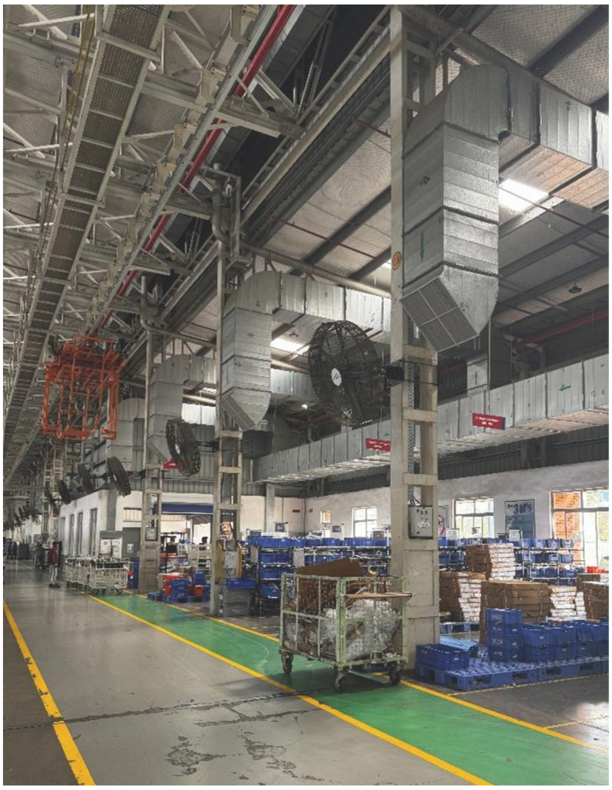

(b)

(c)

(d)

Figure 54. Different HVLS fan locations and Evaporative cooling ducts in Cab Trim and Assembly Shop

LUND UNIVERSITY

Divisions of Energy and Building Design, Building Physics and Building Services

Department of Building and Environmental Technology